U.PORTO

FEUP FACULDADE DE ENGENHARIA
UNIVERSIDADE DO PORTO

AUTOMATED ASSESSMENT OF PARKINSON'S DISEASE FROM GAIT PARAMETERS

MARIA CAROLINA MACHADO DA COSTA PONTES

Dissertation submitted in partial fulfilment of the requirements for the degree of

MASTER IN BIOENGINEERING

Supervisor: Professor João Manual R. S. Tavares

JULY 2026

Dedicated to my family, for all their unconditional support

"The future belongs to those who believe in the beauty of their dreams"

Eleanor Roosevelt

ACKNOWLEDGEMENTS

Ao meu orientador, Professor João Manuel R. S. Tavares, pela disponibilidade e orientação durante a elaboração da dissertação.

À equipa do Laboratório de Estudos de Postura e Marcha da Universidade do Estado de São Paulo, pelo fornecimento do conjunto de dados necessário para o desenvolvimento deste projeto.

Aos meus colegas da FEUP, pelo papel importante que desempenharam durante o meu mestrado, com toda a sua ajuda e apoio.

A todos os professores da FEUP com quem interagi, pois, sem eles, eu não teria adquirido as competências técnicas que me permitiram a realização deste projeto.

Por fim, mas não menos importante, gostaria de agradecer a toda a minha família e aos meus amigos — especialmente aos meus pais e ao meu irmão — por todo o apoio nos bons e maus momentos, por me motivarem e incentivarem a seguir em frente, e por me ajudarem a tornar-me na pessoa que sou hoje.

ABSTRACT

Parkinson's disease (PD) is a neuro degenerative disease caused by the progressive degeneration of the dopaminergic neurons on the substantia nigra of the brain. In the initial stage, occurs the manifestation of non-motor symptoms, such as loss of smell and sleeping disturbances. With the progression of the disease, motor symptoms start to appear, such as bradykinesia, stiffness, tremors, lack of balance and difficulties in movement, which heavily affects the patient's life quality. Currently, there's no cure for PD, and treatments are mainly focused on delaying the symptoms. Early diagnosis plays an important role in the patient's treatment, since starting the treatments sooner might help avoiding the more severe symptoms. However, this is challenging, since diagnosis is usually performed when the motor symptoms appear, that corresponds to a loss of 60 % of dopaminergic neurons. Besides, the diagnosis depends on clinical subjective tests, which contributes to imprecision. Therefore, this dissertation's main objective is the development of a Machine Learning model based on biomechanical gait parameters, to perform the diagnosis of Parkinson's disease. Gait data were collected for four walking conditions, which include for four walking conditions: Free Walking (FrW), Fast Walking (FaW), Dual-Task Walking (DTW), and Obstacle Walking (OBW). Various classifiers were trained on this data, including SVM, LR, DT, RF, NB, XGB, and LSTM.

Several methods of feature engineering were tested, included PSO, SMA and WOA. The algorithms were trained with each of the feature engineering procedures and with the all the features. All the algorithms were evaluated on accuracy, f1-score, recall and precision.

The results of this experiment revealed that the best results were achieved for the XGB model, when all the features were used and the sub dataset for the FaW was used, with an accuracy of 98,61%, a f1 score of 98.59%, a recall of 97.2% and a precision of 100%.

Given the poor performances of the feature engineering models, when compared with the model using al features, future work should pass by incorporating different feature engineering techniques, that are more suited to the dataset used for this work.

KEYWORDS: ML, DL, Parkinson, diagnose, gait.

RESUMO

A doença de Parkinson (DP) é uma doença neurodegenerativa causada pela degeneração progressiva dos neurónios dopaminérgicos na substancia negra do cérebro. Numa fase inicial, ocorre a manifestação de sintomas não motores, como perda de olfato e distúrbios do sono. Com a progressão da doença, sintomas não motores começam a aparecer, nomeadamente bradicinesia, rigidez, tremores, falta de equilíbrio e dificuldades no movimento, o que afeta gravemente a qualidade de vida do paciente. Atualmente não há cura para a DP, e tratamentos focam-se maioritariamente em atrasar os sintomas. Um diagnóstico precoce tem um papel importante no tratamento dos pacientes, visto que iniciar o tratamento mais cedos pode ajudar a evitar os sintomas mais severos. No entanto, isto revela-se desafiador, visto que o diagnóstico é normalmente alcançado aquando do aparecimento dos sintomas motores, que corresponde a uma perda de 60% dos neurónios dopaminérgicos. Além disso, o diagnóstico é dependente de testes clínicos subjetivos, o que contribui para um aumento da imprecisão. Assim, l principal objetivo desta dissertação é o desenvolvimento de um modelo *Machine Learning* baseado em parâmetros biomecânicos da marcha humana, para a realização do diagnóstico de DP. Parâmetros da marcha foram recolhidos para quatro tarefas de marcha: Andar Livre (FrW), Andar rápido (FaW), Tarefa Dupla (DTW) e Andar com Obstáculos (OBW). Vários classificadores foram treinados com estes dados, incluindo: *Support Vector Machine* (SVM), *Logistic Regression* (LR), *Decision Tree* (DT), *Random Forest* (RF), *Naive-Bäyes* (NB), *Extreme Gradient Boosting* (XGB) e *Long-Short Term Memory* (LSTM).

Vários métodos de seleção de características foram testados, nomeadamente *Particle Swarm Optimization* (PSO), *Slime Mould Algorithm* (SMA) e *Whale Optimization Algorithm* (WOA). Os algoritmos foram treinados com cada um dos métodos de seleção de características e com todas as características. Todos os algoritmos foram avaliados de acordo com a *accuracy*, *f1-score*, *recall* e *precision*.

Os resultados desta experiencia revelaram que a melhor performance foi obtida pelo modelo XGB, quando todas as *features* foram usadas e o *dataset* correspondente a FaW foi usado, com uma *accurcy* de 98.61%, um *f1-score* de 98.59%, *recall* de 97.2% e *precision* de 100%.

Considerando a pior performance dos modelos de seleção de características, quando comparados com o modelo que utilizou todas as características, trabalho futuro deverá incluir diferentes técnicas de seleção de características, que sejam mais adequadas ao *dataset* usado para este trabalho.

PALAVRAS-CHAVE: Machine Learning, Deep Learning, Parkinson, diagnóstico, marcha.

TABLE OF CONTENTS

1 INTRODUCTION 1

1.1 MOTIVATION 1

1.2 OBJECTIVES 3

1.3 MAIN CONTRIBUTIONS 4

2 THEORETICAL FUNDAMENTALS 5

2.1 PARKINSON'S DISEASE 5

2.2 DIAGNOSIS 8

2.2.1 Imaging techniques 8

2.3 SYMPTOMS 10

2.3.1 UPDRS 10

2.3.2 Hoehn and Yahr Rating Scale 13

2.3.3 Schwab and England ADL Scale 13

2.4 TREATMENT 14

2.4.1 Pharmacological Treatment 14

2.4.2 Neurosirurgical Treatment 16

2.4.3 Support therapies 17

2.5 BENEFITS OF EARLY TREATMENT 17

2.6 HUMAN GAIT 18

2.6.1 Stance 18

2.6.2 Swing 19

2.6.3 Gait in Parkinson's Disease 20

2.6.4 Gait Parameters 20

2.7 MACHINE LEARNING AND DEEP LEARNING FUNDAMENTALS 21

2.8 DEEP LEARNING 29

3 SYSTEMATIC REVIEW 35

3.1 VOICE AND SPEECH 36

3.2 DRAWING AND HANDWRITING 40
3.3 GAIT 41
3.4 MULTIMODAL DATA 42
3.5 OTHERS 44
3.6 STATISTICAL ANALYSIS 44
4 DATA PREPROCESSING 47
4.1 DATA AUGMENTATION 47
4.2 NORMALIZATION 49
4.3 EVALUATION METRICS 50
4.4 FEATURE ENGINEERING 51
5 METHODOLOGY 55
5.1 DATASET 55
5.2 GAIT TASKS 59
5.2.1 Free Walking 59
5.2.2 Dual Task Walking 60
5.2.3 Obstacle Walking (OBW) 60
5.2.4 Fast Walking 60
5.3 DATA PRE-PROCESSING AND EXTRACTED PARAMETERS 61
5.4 EXPERIMENTAL SETUP 64
5.4.1 Data preparation and splitting 65
5.4.2 Data pre-processing 65
5.4.3 Feature Engeneering 65
5.4.4 Classifier Implementation 66
6 RESULTS AND DISCUSSION 73
6.1 SPATIOTEMPORAL PARAMETERS 76
6.2 DATASET PROCESSING 77

6.3 MODELS RESULTS 79
6.3.1 All features 79
6.3.2 Feature Selection 80
7 CONCLUSION AND FUTURE WORK 86

LIST OF FIGURES

Figure 1- Illustration of the Schwab and England's scale 14
Figure 2- Phases of the gait cycle. Adapted from [25].....19
Figure 3- Schematic representation of gait parameters. Adapted from [28] 21
Figure 4- The worldwide popularity score of various types of ML algorithms in a range from 0 (minimum) to a 100 (maximum) from 2015 to 2020, according to Google Trends. Adapted from [30]. 23
Figure 5- Schematic representation of the different ML models. Adapted from [30]. 23
Figure 6- Schematic representation of a sigmoid decision function 24
Figure 7- Schematic representation of the functioning of the K-Nearest-Neighbour algorithm. Adapted from [31] 25
Figure 8- Example of a separable problem in a 2 dimensional space. Adapted from [30] 26
Figure 9- Decision Tree structure. Adapted from [30].....27
Figure 10- Example of a Random Forrest structure. Adapted from [30].....28
Figure 11- Representation of the structure of an ANN. Adapted from [30].....30
Figure 12- Performance of DL and ML in relation to the amount of data. Adapted from [30] 30
Figure 13- Examples of four different activation functions: sigmoid, hyperbolic tangent, identity, and rectified linear unit. Adapted from [33]. 32
Figure 14- Example of the architecture of a CNN. Adapted from [30] 32
Figure 15- LSTM architecture diagram. Adapted from [34]. 33
Figure 16- Schematic representation of the most used parameters in the development of ML and DL models for PD diagnose 45
Figure 17- Schematic representation of the most used algorithms in the development of ML and DL models for PD diagnose 45
Figure 18-Schematic representation of the most used parameters in the development of multi data-based models for PD diagnose.....46
Figure 19- Illustration of a CTGAN model. Adapted from [40].....49
Figure 20- A) Distribution of participants by sex (female, F; male, M). B) distribution of PD patients by H&Y stage. C) Distribution of participants by age, across groups. D) Distribution of participants by weigh across groups. 58
Figure 21- A) distribution of participants by height (cm) across groups. B) Distribution of participants by MMSA score across groups. C) Distribution of participants by HADS Depression score across groups. D) Distribution of participants by HADS Anxiety score across groups.....59
Figure 22- Complete available data before and after the application of CTGAN 77
Figure 23- Distribution of the spatiotemporal parameters for ObW 78
Figure 24- Distribution of the spatiotemporal parameters for DTW 78
Figure 25- Distribution of the spatiotemporal parameters for FrW 78
Figure 26- Distribution of the spatiotemporal parameters for FaW.....79

Figure 27- Results of the ML and DL models. All the features. 80
Figure 28- Average performance of the models and the sub datasets without feature selection 80
Figure 29- Overall results from applied algorithms after SMA feature selection is applied 81
Figure 30- Overall performance of the models and the sub datasets after SMA feature selection 82
Figure 31- Results obtained by the models after PSO feature selection is applied 83
Figure 32- performance of the algorithms and the datasets after PSO was applied. 83
Figure 33- Results obtained by the models after WOA feature selection is applied. 84
Figure 34- Performance of the algorithms and the datasets after WOA was applied. 84

LIST OF TABLES

Table 1- Resume of the characteristics of the UPDRS subscales 12
Table 2- Resume of the state of the Art. Voice and Speech 37
Table 3- Resume of the state of the Art. Drawing and Handwriting 40
Table 4- Resume of the state of the Art. Gait analysis 41
Table 5- Resume of the state of the Art. Multimodal data....42
Table 6- Resume of the state of the Art. Other symptoms....44
Table 7- Demographic parameters of the PD patients and the HC group. 56
Table 8- Feature selection with PSO 62
Table 9- Feature selection with SMA....63
Table 10- Feature Selection with WOA....63
Table 11- Hyperparamters of the SVC classifier 66
Table 12- Hyperparameteres for the KNN classifier....67
Table 13- Hyperparameteres for the DT classifier....68
Table 14- Hyperparameteres for the RF classifier....69
Table 15- Hyperparameters of the GaussianNB classifier....69
Table 16- Hyperparameters of the LR classifier....70
Table 17- Hyperparameters used for the LSTM classifier....71
Table 18- Gait parameters, ObW....73
Table 19- Gait parameters, FrW....74
Table 20- Gait parameters, DTW....74
Table 21- Gait parameters, FaW 76

SYMBOLS, ACRONYMS AND ABBREVIATIONS

PD	Parkinson's Disease
FoG	Freezing of Gait
ML	Machine Learning
DL	Deep Learning
SNpc	Substantia nigra pars compacta
LB	Lewy-bodies
α-Syn	α-Synuclein
REM	Rapid Eye Movement
SPECT	Single photon emission computes tomography
TC	Transcranial sonography
PET	Positron emission tomography
MRI	Magnetic Resonance Imaging
CT	Computed tomography
MRS	Magnetic resonance spectroscopy
UPDRS	*Unified Parkinson Disease Rating Scale*
H&Y	*Hoehn and Yahr Rating Scale*
CDS	Continuous dopaminergic stimulation
COMT	Catechol-O-methyl
MAO-B	monoamine oxidase aldehyde dehydrogenase B
DBS	Deep Brain Stimulation
VIM	Ventral intermediate nucleus (VIM
STN	Subthalamic nucleous
GPi	Globus palidus internal
AI	Artificial Intelligence
NB	Naïve Bayes
LDA	Linear discriminant analysis
LR	Linear Regression

KNN	K- Nearest- Neighbour
SVM	Support Vector Machine
RBF	Radial Basis Function
DT	Decision Tree
RF	Random Forest
AdaBoost	Adaptive Boosting
XGB	Extreme Gradient Boosting
CatBoost	Categorical Boosting
ANN	artificial neural networks
MLP	Multi-Layer Perceptron
CNN	Convolutional Neural Networks
LSTM	Long Short-Term Memory
2D	Two dimensional
VGG	Visual Geometry Gorup
RNN	recurrent neural network
GWO	Grey Wolf Optimization
DNN	Deep Neural Network
GB	Gradient Boosting
LSTM	Long-Short-Term-Memory
LGBM	Light Gradient Boosting Machine
SVC	Support Vector Classification
FCNN	Fuzzy- Convolutional Neural Networks
FKNN	Fuzzy K-Nearest Neighbour
DBN	Deep Belief Network
XAI	Explainable Artificial Intelligence
ET	Evapotranspiration
GNB	Gaussian Naïve Bayes
GNN	Graph Neural Networks
EM	Expectation Maximization

RMS	Root Mean Square
RAE	Relative Absolute Error
RSE	Research Software Engineer
CTSO-ZFNet	Chronological Tangent Search Optimization-Zeiler and Fergus Network
STFP	Short-Term Traffic Flow Prediction
TCN	Temporal Convolutional Networks
FNN	Feedforward Neural Network
AEO	Answer Engine Optimization
GRU	Gated Recurrent Unit
Min	Minimum
Max	Maximum
TP	True Positive
TN	True Negative
FP	False Positive
FN	False Negative
Acc	Accuracy
Rec	Recall
F1	F1-score
Pres	Precision
CTGAN	Conditional Tabular Generative Adversarial Network
SMOTE	Synthetic Minority Over-sampling Technique
FrW	Free Walking
DTW	Dual Task Walking
OBW	Obstacle walking
FaW	Fast Walking
MMSE	Mini Mental State Examination
HC	Healthy Control
HADS	Hospital Anxiety and Depression Scale
PSO	Particle Swarm Optimization

SMA	Slime Mould Algorithm
WOA	Whale Optimization Algorithm

1
INTRODUCTION

1.1 MOTIVATION

Parkinson' Disease (PD) is the second most incident neuro degenerative disease in the world, after Alzheimer. In the past years, it presented an elevated growth, in prevalence, incapacity and death. The average age for the beginning of the disease is 60, and the average life expectancy after diagnosis is 15 years

On the initial stage, it presents non-motor symptoms that might precede the motor symptoms by years or even decades. One of the most common non-motor symptoms is the loss of smell. Recent studies show that about 95 % of patients diagnosed with PD suffer of some kind of loss of smell in the time of the diagnosis. Other common non-motor symptoms may include dementia, depression, apathy and sleep disturbances, with 98 % of patients diagnosed with PD presenting at least one of these symptoms

Concerning the motor symptoms, the most common ones are bradykinesia, stiffness, tremors and difficulty in posture and movement. • Bradykinesia is a requisite to the diagnose of PD, according to the criteria defined by UK Parkinson's Disease Society Brain Bank. It's described as a decrease in the speed of initiation of voluntary movements, with a progressive reduction in the capacity of providing enough energy to the muscles. This leads to difficulty in executing sudden moves, response reactions, or executing several actions at the same time. This symptom is recognizable in activities that require an elevated motor control, such as writing, facial expressions, speaking and swallowing

Stiffness is defined as lack of flexibility in the muscles. This limits the movements that might be executed. Stiffness may also lead to musculoskeletal pain, which may be confused with arthritis

Tremor is one of the most common and recognizable symptoms of PD. Consists in the rhythmic extension and distension of the muscles. Usually it's manifested in the extremities of the body, such as hands and feet, but it may also spread to the hips or 3 jaw. Tremors might be present both in resting and during the execution of motor activities

Posture instability appears in the most advanced stage of the disease, and has a big impact on the patient's life, since it might lead to falls or fractures. It's unresponsive to dopaminergic therapies

The absence of defined biomarkers and conclusive diagnostic tests makes the execution of a precise diagnose more difficult. Health care professionals base mostly on motor symptoms, such as bradykinesia, tremors, muscle stiffness and changes in posture. However, these symptoms appear in a more advanced stage of the disease, equivalent to a loss of 60 % of the dopaminergic neurons, and might overlap with the symptoms of other diseases, which increases the difficulty of a precise diagnose. Despite pre-motor symptoms preceding the clinical diagnosis, none of these are sufficiently specific to be used as stand-alone biomarkers. The probability of misdiagnosis is also strongly related to who is doing the diagnosing, and the diagnostic criteria applied. Studies show that about 47 % of PD diagnosis in primary care are incorrect, while diagnosis made by movement specialists are incorrect only 6% to 8 % of the times. Wrong diagnosis might lead to wrong treatments that might cause damages to the patient. Therefore, it's necessary to have accurate and objective diagnosis which doesn't rely on clinical subjectivity. Taking this into account, several proposals of Machine Learning Models based on biomechanical data that aim to diagnose PD have been appearing. Human gait refers to any movement that allows moving from one place to another. This process suffers modifications in individuals with PD, which makes it a useful parameter in diagnosis.

The typical walking pattern for patients with PD includes dragged walking, with decreased speed, smaller length of the steps, smaller angular velocity and less swing of the arms. This is due to symptoms as bradykinesia and stiffness of the muscles that prevent the selective deactivation of the muscle during movement. Posture also suffers alterations, as the trunk leans forward, the head leans down and the knees, hips, elbows and ankles bend, although this symptom happens in more advanced stages of the disease. In general, patients also experience an increased difficulty in starting movement, often experiencing freezing of gait (FoG). FoG is characterized by a blocking of the movement, due to lack of movement in the feet that appear to be stuck to the floor. It also becomes harder to move direction, as patients round as one single stiff unit

The alterations on the gait appear very soon and tend to get worse with the progression of the disease, which means that the analysing of the gait provides information about the stage of the disease as well. Currently, there's no cure for PD, and treatments mainly focus on relieving symptoms. There are three main ways of treatment: pharmacologic, neuro surgical and supporting therapies.

Pharmacological treatment is essentially made with dopamine based medication, aiming to rebuild dopaminergic functions in the brain. Levodopa is the standard medication. However, as the disease progresses, the brain loses its ability to storage dopamine, which leads to the induction of motor complications, such as dyskinesia. Dyskinesia is characterized by involuntary movements of the limbs, trunk and head. Around 80 % of patients with PD experience dyskinesia induced by levodopa in advanced stages of the disease. Therefore, current treatments include other medication used along with levodopa, to correct possible secondary effects.

1.2 OBJECTIVES

This dissertation's main objective is the development of a Machine Learning algorithm capable of performing the diagnoses of Parkinson's Disease based on biomechanical data of the human gait, as well as providing information about the stage of progression of the disease. Additionally, a systematic review of the currently existing ML models that perform the diagnosis of PD will be executed, as well as the development of data augmentation and outlier removal methods.

1.3 MAIN CONTRIBUTIONS

The main contributions made by this thesis, both scientific and methodological, to the field of PD detection using gait analysis and ML/DL are summarized below:

Systematic Review of ML and DL Approaches for PD Detection using gait parameters

- Conducted a systematic review of machine learning and deep learning approaches for Parkinson's disease detection using gait as a digital biomarker.
- Mapped and compared model types, dataset characteristics, and evaluation methodologies across the literature.
- Identified methodological trends, current limitations, and open challenges, outlining future research needs in multimodal data fusion, robust validation, and clinical translation.

2
THEORETICAL FUNDAMENTALS

2.1 PARKINSON'S DISEASE

Parkinson's Disease (PD) is the second most common neurodegenerative disease in the world. PD is caused by a progressive loss of dopaminergic neurons in the midbrain substantia nigra pars compacta (SN*pc*), which is part of the basal ganglia, the brain region responsible for motor controls, and the accumulation of characteristic eosinophilic inclusions known as Lewy-bodies (LBs), containing misfolded protein aggregates including α-Synuclein (α-Syn) in those dying dopaminergic neurons [1]. Dopamine is a neurotransmitter produced by the dopaminergic neurons responsible for the transmission of signals from the central nervous system to the motor neurons of the peripheral neural system. Therefore, the decrease of dopamine levels affects the correct execution of movements [2].

PD was first described by James Parkinson in 1817 in "An Essay on the Shaking Palsy as a specific syndrome. PD is clinically characterized by both motor and non-motor symptoms that might precede the motor symptoms in years or even decades. The most common motor symptoms include [3]:

- Tremor. Rest tremor is one of the most common and easily recognizable symptoms of PD. Tremors are typically unilateral and occur at a frequency between 4 and 6 Hz. Initially, tremor is almost always observed in the distal part of an extremity and is most prominent when the limb is in poster of repose. While less common, the head, jaw, and tongue may be involved, but, unlike essential tremors, rarely involves the neck/head or voice [3] [4].
- Bradykinesia. Refers to the slowing of movement and the simplification of complex motor tasks. This causes a decrease in spontaneous movements and in the ability of performing several tasks at the same time, which causes alterations in activities that

require an elevated motor control. The blinking rate decreases, and the facial muscles move less, which makes the face appear more emotive. Speech becomes softer and monotone, and spontaneous swallowing is reduced. Limb movements become more restricted, with a decreased amplitude, and frequent occurrences of freezing of movement. This causes alterations in handwriting and in the patient's gait, that might lead to fall [3] [4].

- Stiffness. Stiffness is defined as the loss of flexibility in the muscles, which translates into an increased resistance to movement. Stiffness is also associated with pain. Painful shoulder is one of the most common initial manifestations of PD, but is often misdiagnosed as arthritis, bursitis or rotator cuff injury [4].
- Alterations in posture. The increased rigidity in the trunk and neck might lead to alterations in posture, namely flexed neck, trunk, elbows and knees. However, flexed posture generally happens in advanced stages of the disease. In some cases, striatal limb deformities (e.g., striatal hands and striatal toes) may also occur. Patients that experience striatal deformities are generally younger and experience parkinsonian symptoms sooner. Other skeletal deformities include extreme neck flexion (''dropped head'' or ''bent spine''), truncal flexion (camptocormia) and scoliosis. Camptocormia is exacerbated by walking and relieved by sitting, lying in the supine position or extending the trunk [4].
- Freezing. Freezing manifest a sudden and transient inability to move. There are five described subtypes of freezing: start hesitation, turn hesitation, hesitation in tight quarters, destination hesitation and open space hesitation. Freezing, also referred as motor blocks, is more common in men than in women, and less common in patients whose main symptom is tremor. Freezing usually affects the legs during walking, causing freezing of gait, but the arms and eyelids can also be involved [4].

Non motor symptoms

Non motor symptoms are a common and often underappreciated symptom of PD, and can be as debilitating as motor symptoms. These include

- Anosmia, i.e., loss of the sense of smell. This is a very common non motor symptom associated with PD. Recent studies show that about 90 % of patients diagnosed with PD suffer of some kind of loss of smell in the time of the diagnosis.
- Dysautonomia. A very common symptom, presented by virtually every PD patients. Dysautonomia refers to conditions that affect the peripheral autonomic nervous system, responsible for regulation of the automatic, involuntary processes of the body, such as heart rate, blood pressure and digestion [5] [6]. Common symptoms of dysautonomia experienced by PD patients include gastrointestinal complaints, such as constipation (a very early symptom), bloating, nausea and abdominal discomfort.
- Cognitive decline and dementia. Cognitive decline is defined as a decrease in multiple cognitive domains, including memory, reasoning and processing speed [7]. The Sydney Multicentre Study of PD found that 84% of patients with PD evaluated show

cognitive decline and that 48% met the diagnosis for dementia after a 15 year follow-up. PD dementia is also associated with several other neurological disorders, including depression, anxiety, apathy and hallucinations.

- Depression. Depression is a clinical mood disorder that causes a persisted feeling of sadness and loss of interest. Depressive disorders are classified into 5 types, according to The American Psychiatric Association's Diagnostic Statistical Manual of Mental Disorders, Fifth Edition (DSM-5): Disruptive mood dysregulation disorder; Major depressive disorder; Persistent depressive disorder (dysthymia); Premenstrual dysphoric disorder; and Depressive disorder due to another medical condition, such as PD. The common features of all depressive states include sadness, emptiness, or irritable mood, accompanied by somatic and cognitive changes that significantly affect the individual's capacity to function [8].
- Anxiety. Anxiety is an emotion characterized by apprehension and somatic symptoms of tension in which an individual anticipates impending danger, catastrophe or misfortune and the body mobilizes itself to meet the perceived threat. Common symptoms if anxiety include tension in the muscles, faster breathing and accelerated heartbeat [9].
- Sleep Disturbances. Sleep disturbances are a common symptom of PD patients, affecting 88% of dwelling patients, that have a high impact on the decrease of the quality of life. Disturbances on sleep might result in excessive daytime sleepiness and poor daytime functioning, as well as lack of enthusiasm for daytime activities. Adverse effects might also be caused to the spousal caregiver. Insomnia is a common sleeping disturbance and is defined as an almost nightly complaint of an insufficient amount of sleep or feeling unrested after sleep [10]. Rapid Eye Movement (REM) is also common, occurring in around one third of patients with PD. REM is nowadays considered a pre-parkinsonian state, and is characterized by an increase in violent dream content, accompanied by talking, yelling, swearing, grabbing, punching, kicking, jumping and other dramatic, violent and potentially injurious motor activity which may also involve the bed partner. The sleep abnormalities observed in patients with PD may possibly be related to a 50% loss of hypocrite (orexin) neurons. [4].
- Psychosis. It's the leading cause for nursing home placement of PD patients and one of the factors that increases the risk of mortality. Psychotic features arise later in the disease and manifest as visual hallucinations, minor sensory disturbances and paranoid delusions. Symptoms tend to worse with the progression of the disease, and insight is ultimately lost [11].
- Sensory abnormalities. Sensory symptoms recognized as parkinsonian symptoms include olfactory dysfunction, pain, paraesthesia, akathisia, oral pain and genital pain [4].

Studies show that 98% of patients diagnosed with PD present at least one of these symptoms [3] [12].

2.2 DIAGNOSIS

Diagnosis of PD in clinical practice is primarily based on the presence of cardinal motor features, associated and exclusionary symptoms, and response to levodopa. Neuroimaging techniques and specific biomarkers are important to achieve early diagnosis as well.

2.2.1 Imaging techniques

Several neuroimaging techniques have proven viable in the detection of PD, and are therefore good complementary tools to achieve an early diagnosis. The most common techniques include single photon emission computes tomography (SPECT), transcranial sonography (TCS), positron emission tomography (PET) and magnetic resonance imaging (MRI) [13].

SPECT is a nuclear imaging modality, widely used in clinical applications. It creates a 3 dimensional image of the distribution of a radioactive tracer, that might be called a probe, injected into the bloodstream and subsequently taken up by certain tissues. Apart from purely anatomic imaging modalities, such as CT and MRI, SEPCT allows the clinician to access the tissues functionality and physiology, and is more accessible and less expensive to clinicians than PET. However, it doesn't allow for the distinction between PD and other neurodegenerative disease, such as multisystem atrophy, progressive supranuclear palsy and corticobasal degeneration [13] [14].

TCS is a neuroimaging technique that displays the brain parenchyma and the intracranial ventricular system through the intact skull [15]. It employs low frequency acoustic waves through the temporal bone window, which allows the visualization of the echogenicity of human brain tissue [16]. The different imaging principle applied in this technique allows for a better image resolution of the echogenic brain structures, not only in comparison with former imaging techniques, but also compared to MRI, under clinical conditions. Other advantages of TCS include on-time dynamic imaging, relatively low costs and wide availability, when compared to other imaging methods, such as PET, short investigation time, noninvasively and unlimited repeatability, mobility, bedside availability and little corruptions by patients' movements [17]. TCS is a particular useful tool to the analysis of the characteristic changes in neurodegenerative diseases, such as the hyper echogenicity of the substantia nigra in PD patients. Particular, TCS is useful in the differentiation of idiopathic Parkinson's disease from other parkinsonian disorders [17]. The main limitations of this technique are the insufficient temporal bone window (5% -20% of patients) and its dependency on the experience and skill of the investigator [17]. Additionally, TCS imaging conditions are more difficult in adults, due to the thickening of the temporal bone with increasing of age [15].

MRI is a non-invasive imaging technique that generates cross-sectional images of internal structures, by using nonionizing electromagnetic radiation. MRI is incredibly versatile, and can provide information regarding the tissue's biochemistry and gross structural properties, as well as augment the factors of interest, by tailoring the techniques used to analyse the signal, which allows obtaining high-resolution images of particular structures. Therefore, MRI provides multi-parameter information on brain anatomy, function and metabolism [18]. MRI is a particularly good alternative to methods previously mentioned for patients with atypical clinical features for PD [13].

In vivo magnetic resonance spectroscopy (MRS) is an additional tool that might be used to complement MRI. MRS is useful to detect metabolic changes of the brain in patients with PD and has been shown to match the criteria of an ideal imaging biomarker. The main benefits of this technique are its availability and low cost, when compared to other imaging techniques, such as PET and SPECT, and its consistency. Additionally, MRS is not bounded to specialized centres, making it more accessible to general public health centres, and does not require a contrast agent, which decreases exposure to radioactive substances. Studies have shown MRS ability to reach a differential diagnosis of PD from other forms of parkinsonism, especially in the early stages when many of the symptoms overlap [13].

In addition to being useful diagnostic tools, these imaging techniques can also be used to monitor disease progression [13].

2.2.2 Biological and genetic biomarkers

Several biological indicators have been proposed for use in the diagnose of PD, including cerebrospinal fluid, blood and urine. The main limitations regarding the use of biomarkers revolves around the fact that their presence and measurable levels change with the progression of the disease. Moreover, the manifestations of biomarkers of other disease that cause cognitive impairment might be too similar, which decreases the ability of an accurate differentiated diagnose [13].

2.3 SYMPTOMS

Although a definitive diagnosis of PD can only be achieved by a brain autopsy, a clinical diagnosis might be obtained based on both motor and non-motor symptoms. There are several different scales used to access different manifestations of PD. Some of the most known ones include the ***Unified Parkinson Disease Rating Scale*** **(UPDRS)**, the ***Hoehn and Yahr Rating Scale*** and ***Schwab and England ADL Scale***.

2.3.1 UPDRS

The UPDRS has the great acceptance as a tool for diagnose and follow up of patients. The current UPDRS includes four subscales, where subscale one evaluates mentation, behaviour and mood, subscale two rates activities of daily life, subscale three rates motor manifestations, and subscale four covers complications of therapy [19].

Subscale I consists of questions regarding intellectual impairment, though disorder, depression and motivation and initiative. Scores ranging from 0 to 4 are attributed to the patient's answers, with 4 representing the greatest level of dysfunction. The sum of the total scores for this subscale can range from 0 to 16 [19].

Subscale II evaluates activities of daily living. The examiner asks the patient to describe his or her function in the ON and OFF state. Each of the 14 items in subscale II is given a score that ranges from 0 to 4, where 4 equals most dysfunctional. Each item is scored twice, for the ON and the OFF phase. The total score of this subscale ranges between 0 and 56 [19].

Subscale III is an examiner rate of the motor manifestations of PD, and is the most commonly used subscale. This subscale contains 14 different types of ratings, with many of these ratings done for each limb separately. Each rating ranges from 0 to 4, with the total score ranging from 0 to 108. The original UPDRS scale only used integers, but currently, some use increments of 0.5. This subscale contains 27 observations, that evaluate tremor at rest, action tremor, rigidity, bradykinesia, speech, facial expressions, posture, posture instability, gait, and arising from a chair. Tremor at rest and rigidity are evaluated separately in the face and each extremity, while action tremor is evaluated separately for each hand and bradykinesia is rated through three different methods in the upper extremities, rating left and right separately, in the feet and in the body [19].

Subscale IV rates complications in therapy. It contains eleven questions that relate to the observations of the patient or caregiver during the preceding week. Questions 1 to 3 and 8 are rated from 0 to 4, but the others are simply yes or no questions. The score of this subscale ranges from 0 to 23. This subscale makes a crude measurement of dyskinesias, and, therefore, own of the main limitations is that it relies on the patient's own perception, since the patients might not realize they are having dyskinesias. In this situation, it's useful to interview a caregiver or other observer to obtain collateral information [19].

A resume of the subscales of UPDRS, the rated items and their scores can be found in Table 1.

Table 1- Resume of the characteristics of the UPDRS subscales

Subscale	**Evaluated Characteristics**	**Items**	**Score Range**
Subscale I	Mentation, behaviour and mood	Intellectual impairment Though disorder Depression Motivation and initiative	0 to 16
Subscale II	Activities of daily living	Speech Salivation Swallowing Cutting food and handling utensils Dressing Hygiene Turning in bed and adjusting bedclothes Falling (unrelated to freezing) Freezing when walking Walking Tremor in right arm Tremor in left arm Sensory complaints related to parkinsonism	0 to 56
Subscale III	Motor examination	Tremor at rest, in the face and each extremity (5 ratings) Action tremor, for both hands separately (2 ratings) Rigidity, for the neck and all four extremities separately (5 ratings) Bradykinesia, finger tapping, for left and right upper extremities separately (2 ratings). Bradykinesia, opening and closing hand, for both hands separately (2 ratings) Bradykinesia, rise elbow, for both arms (2 ratings) Bradykinesia, rise foot, for both feet separately (2 ratings) Speech Facial expressions Arising from a chair Gait Posture Postural stability Body bradykinesia	0 to 108
Subscale IV	Complications of therapy	Dyskinesias Disability Pain Early morning dystonia Predictability of OFF periods Unpredictability of OFF periods Sudden OFF periods Duration of OFF periods GI complaints Sleep disturbances Orthostatic	0 to 23

2.3.2 Hoehn and Yahr Rating Scale

The Hoehn and Yahr staging was first described in 1967 and consists of a simple staging, from 1 to 5, of the motor manifestations of PD, intended to reflect the degree of progression. It combines features of motor impairment and disability. However, this scale is not linear and might not even be ranked order, as someone with substantial bradykinesia but good stability on the pull test would be on stage 2, having more disability than someone ranked on stage 3 that fell on the pull test but has relatively mild bradykinesia and rigidity, for instance. The rating was modified to include two half scores, but no clinometric test of this modification has been done. Overall, this staging is best used for subject description groups, and analysis should involve non parametric statistics. This rating is based upon examination, according to the following criteria [19]:

- 0- no signs of the disease;
- 1- unilateral disease (on one side);
- 1.5- unilateral disease plus axial involvement;
- 2- bilateral disease, without impairment of balance;
- 2.5- bilateral disease, with recovery on the pull test;
- 3- mild to moderate bilateral disease; needs assistance to prevent falling on pull test; physically independent;
- 4- severe disability, but still able to walk or stand unassisted;
- 5- wheelchair-bound or bedridden unless aided;

The pull test is done to access an individual's postural stability. The patient is asked to stand with the feet shoulder width apart and eyes open. The examiner stands behind the patients and instructs to patient to resist a backwards pull, but, if necessary, to take a few steps back to maintain balance. The examiner gives a strong backwards pull on the patient's shoulders, and verifies if the patient manages to maintain balance [19].

2.3.3 Schwab and England ADL Scale

The Schwab and England's scale is used to access the patient's ability to perform activities of daily living (ADL). The rating is done by having the examiner interviewing the patient and, frequently, a collateral source, such as a spouse or a caregiver. This rating varies from 0 to 100% with 5 % increments [19]. A representation of this scale can be found in Figure 1.

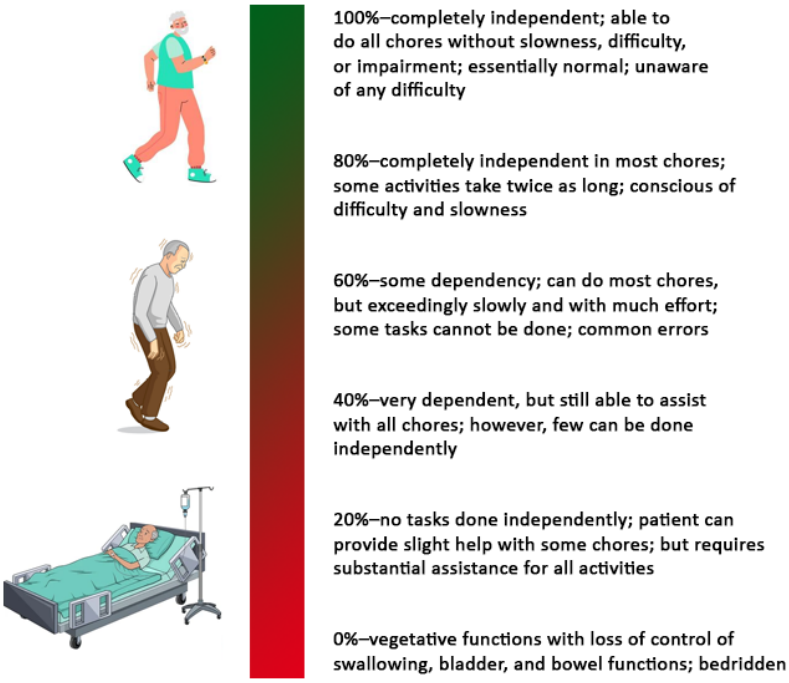


Figure 1- Illustration of the Schwab and England's scale

2.4 TREATMENT

Currently, there's no known therapy that can slow down or arrest PD progression, and most therapies focus on relieving the symptoms in order to minimize the disease's impact on the patient's daily life. Therefore, treatment options must be individualized and tailored to the needs of each individual patient.

2.4.1 Pharmacological Treatment

2.4.1.1 levodopa

A great progress has been made in the treatment of PD in the past half century, but levodopa remains the standards therapy for motor control of PD and it's still considered the most effective drug for relieving the widest range of symptoms, particularly symptoms related to bradykinesia. It is the immediate precursor to dopamine, which can cross the blood-brain barrier. It allows the depleted number of dopaminergic neurons to produce more dopamine and alleviate symptoms.

Although levodopa is the most widely used and effective therapy for PD, its utilization is associated with motor complications in the majority of patients, such as motor fluctuations ("wearing off" effect) and dyskinesias (involuntary writhing movements), and other side effects, including nausea, vomiting, hallucinations, delusions, somnolence and dystonia. Dyskinesias constitute the main limiting of the dosage and duration of the L-dopa treatment [3] [20].

Several drugs have been reported to improve the levodopa associated motor complications, without the need to decrease the dosage. The addition of a COMT inhibitor, MAO-I inhibitor or and dopamine agonist inhibitor is useful in the management of levodopa induced motor fluctuations. Other drugs with antidyskinetic effect include clozapine, fluoxetine, propranolol, the cannabinoid receptor agonist nabilone, and fipamezol. In patients with severe motor fluctuations, apomorphine, a subcutaneous dopamine agonist, may be used as rescue therapy [20]. Levodopa is also often paired with carbidopa, a peripheral dopa decarboxylase inhibitor that blocks metabolism of levodopa in the periphery, increasing central nervous system bioavailability and lessening peripheral side effects, particularly nausea [3].

Increasing the frequency of administration of levodopa is also used to improve motor fluctuations experienced by patients. Slow release preparations of levodopa allow the possibility of "smoothing out" clinical fluctuations by slowly releasing levodopa from a special matrix. Continuous dopaminergic stimulation (CDS) has also been advocated as a strategy to control motor fluctuations. CDS methods include duodenal infusions, oral solutions, subcutaneous or intramuscular injections, among others [20].

2.4.1.2 Dopamine agonists

Dopamine agonists directly activate dopamine receptors, bypassing the presynaptic synthesis. DA agonists offer only modest improvement, and are mainly used in early stages of the disease to delay the introduction of levodopa, in order to prevent levodopa associated complications [20].

Catechol-O-methyl (COMT) inhibitors, such as entacapone, and monoamine oxidase aldehyde dehydrogenase B (MAO-B) inhibitors, such as rasagiline and selegiline, inhibit enzymes involved in the breakdown of levodopa and dopamine, prolonging the effect of carbidopa/levodopa. However, they might also increase the side effects of levodopa, principally hallucinations, dyskinesia and nausea.

2.4.1.3 Non- dopaminergic therapy

No dopaminergic drugs, such as anticholinergics and amantadine may provide satisfactory symptom relieve in early stages of PD, as they stimulate dopaminergic receptors in the central nervous system, and carry a lesser risk to cause dyskinesias. However, the decreased specificity causes an increased risk of hallucinations, hypotension, somnolence (sometimes with sleep attacks), leg edema, and the risk of compulsive behaviours. Besides, anticholinergics aren't effective for treating bradykinesia, are mostly used for younger patients whose early manifestations are rigidity and tremor. They are also limited by their side effects, such as cognitive impairment, dry mouth and urinary symptoms [3] [20].

Antipsychotics are sometimes necessary to treat symptoms like hallucinations and paranoid delusions. The most well tolerated agents include quetiapine, clozapine and pimavanserin [3].

Antidepresssives are often used as well, since depression is a frequent symptom of PD patients. Tricyclic antidepressants, serotoninnoradrenaline reuptake inhibitors, or serotonin reuptake inhibitors have all been used [3].

2.4.2 Neurosirurgical Treatment

Deep Brain Stimulation (DBS) has become a staple in treatment of PD patients that don't respond well to other treatments. DBS is achieved with the implementation of stimulating electrodes in the ventral intermediate nucleus (VIM) of the thalamus, subthalamic nucleous (STN), globus palidus internal (GPi) or other subcortical nuclei, with STN stimulation being the most common modality used in the treatment of PD [20] [21]. The exact mechanism responsible for the clinical effects of DBS is still under debate. Experimental work has suggested that DBS (of STN) interacts with the diseased neural networks, exciting some pathways while inhibiting others to eliminate or subdue the underlying pathological neural activity in the basal ganglia [21].

Several studies have reported the efficacy of DBS in reducing dyskinesias, improving motor performance, reducing the requirement for dopaminergic medication, increasing independence in activities of daily living, and improving quality of life. However, like any surgical procedures, DBS might be associated with several complications, including intracerebral haemorrhage, infections, foreign body intolerance, among others. Besides, although DBS brings sustained benefits for PD patients that go through this procedure, studies show that patients slowly deteriorate over time, and a majority develops severe no motor and axial symptoms. This proves that, in spite of being able to relieve symptoms in an early stage of the disease, DBS is unable to stop the progression of the neurodegenerative process that happens in the brain of PD patients [21].

2.4.3 Support therapies

Support therapies are used as a complement to other treatments and, unlike conventional therapies, don't focus on treating the underlying cause of motor symptoms, but rather on managing symptoms, in order to improve the patient's daily life [22]. These therapies include exercise, physiotherapy, occupational therapy, speech and language therapy and neuro-rehabilitation. More unconventional therapies, like dance, music therapy and mindfulness, have also been explored [13].

2.5 BENEFITS OF EARLY TREATMENT

The diagnosis of PD often occur when the disease is in an advanced stage, in which motor symptoms are clearly evident and neurophysiological damages have taken place, affecting the patient's quality of life. Several studies have pointed to the advantage associated with early therapeutic intervention in PD [23].

The most significant benefit of early intervention is the reduction of symptoms and the slowing of the disease progression. An intervention during the early stage of PD also allows a delay of the levodopa initiation, since other less potent drugs can be used to alleviate minor symptoms. This leads to a reduction of the levodopa associated complications, such motor fluctuations and dyskinesias. Clinical trial suggest, but have yet to conclusively prove, that an early intervention can slow the disease progression, improving the patient's quality of life and life expectancy [23].

Regarding the direct costs associated with PD, the estimated annual costs of PD in Europe are €14 billion [24], with the great majority of costs related to the more advanced stages of the disease, when the symptoms are most severe. Therefore, an early intervention that manages to slow the disease progression and diminish symptoms could have a significant impact in decreasing PD related expenditures [23].

Early diagnosis also plays an important role in scientific investigation of new treatments, as the accompanying of patients with PD since an early stage may provide more information about the alterations that occur in the nervous system of the diagnosed patients.

2.6 HUMAN GAIT

Human gait is defined as "a series of movements of the lower extremities in such a rhythmic motion that result in the forward progression of the body" [25]. Walking is the most commonly used form of gait, followed by running. Human gait is a fundamental key to in the environment and, therefore, normal gait is critical to an individual's quality of life. Normal gait is both steady and flexible, resulting in a steady movement, while also allowing for change in speed and manoeuvring in different soil conditions [26].

Gait can essentially be divided in two phases: swing and stance [27]. These are segregated into eight sub-phases [25].

2.6.1 Stance

The stance phase consists of 60 % of the gait cycle. It's divided into 4 sub-phases [25]:

- Initial Contact. This is the phase when the foot comes in touch with the floor. The limb's loading response is determined by the joint's positions during this phase [25].
- Loading Response. The beginning of this phase is marked with the foot's initial contact with the floor, until the other foot is ready for swing or is lifted for a wing. For shock absorption, the knee is flexed and the heel is used as a rocker, while with the contact of the forefoot, the heel rocker is limited with the ankle flexion [25].
- Midstance. In this phase, the limb advances forward over the stationary foot, with the rocker of the ankle. The midstance phase begins with the lift of the foot, and ends when the body's weight aligns on the forefoot [25].
- Termineal stance. This phase begins with the heel rise of the foot and ends when the other foot hits. The forefoot rocker leads to the advancement of the limb, and the body's weight shifts ahead of the forefoot [25].

2.6.2 Swing

The swing phase takes 40 % of the gait cycle, and it's divided into 4 sub-phases as well [25]:

- Pre-swing. This phase begins with the initial contact of the other limb, and ends with the toe-off [25].
- Initial swing. This comprises one third of the swing phase. It begins with lifting the foot from the floor and ends when the stance foot is opposite the swinging foot [25].
- Mid-swing. In the beginning of this phase the stance limb is opposite to the swinging limb, while the ending occurs when the tibia is vertical, and the swinging limb is forward [25].
- Terminal swing. This phase begins with the swing of the vertically positioned tibia and ends with the strike of the foot on the floor. The limb movement is completed when the shank moves ahead of the thigh, accompanied by the knee extension [25].

A schematic review of the phases of the gait cycle can be seen in Figure 2.

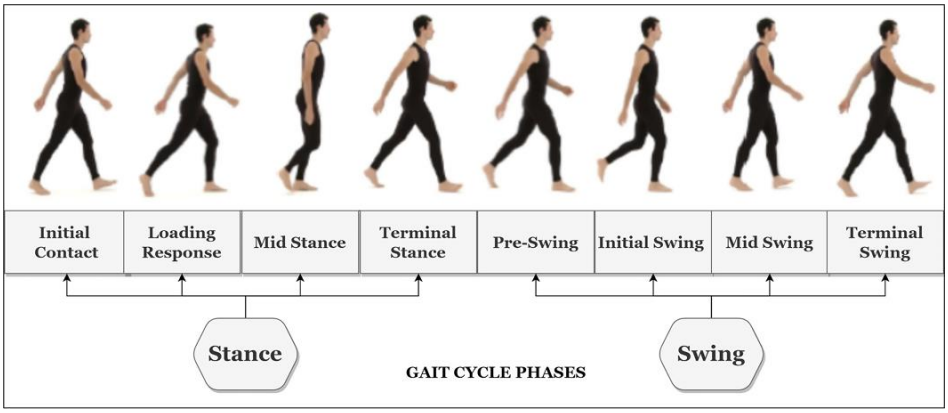


Figure 2- Phases of the gait cycle. Adapted from [25]

2.6.3 Gait in Parkinson's Disease

For a patient diagnosed with PD, changes in gait are noted. Frequently, there's a decrease in arm swing that is usually asymmetrical, or a disappearance of arm swing altogether, a decrease in gait speed, and shortening of the step length [28]. The length of the patient's stride diminishes, and turn on pivot becomes progressively more difficult, which leads to the patient having to turn "*en bloc*", using several small steps. Eventually, the patient might develop propulsion or retropulsion. Postural instability may also occur, with the trunk getting ahead of the feet, leading to a necessity to take small running steps, in order to allow the patient to regain balance [3]. This increases the chances of falling, which carries the risk of fractures and injuries. In the later stages, it may also occur episodes of freezing of gait. Freezing of gait (FoG) is an episodic phenomenon characterized by an inability to step, or only being able to take small steps (with only a few millimetres or centimetres length), despite the intention to walk. A subjective feeling of the foot being glued to the ground, and a trembling of the legs at a rate of 3-8 Hz usually accompanies episodes of FoG. FoG can be asymmetrical, affecting mainly one foot or being elicited more easily by turning in one direction [29].

2.6.4 Gait Parameters

- In order to make a proper analysis of the patient's gait, it's imperative to have a detailed understanding of the gait parameters, their usual values and the changes these parameters undergo in PD patients. Patio- temporal parameters include:
- Walking velocity; Walking velocity can be defined as the distance covered by unit of time [25].
- Step length; Step length is defined as the distance between consecutive heel contact points of opposite feet. Unequal step length serves as an indicator of a gait abnormality [25].
- Stride length; It is defined as the distance between two heel contact points of the same foot [25].
- Single limb support. It expresses the percentage of the gait cycle spent on expressed limb. This measurement is related to the knee joint, and its value decreases the patient experiences an injury in the knee [25].
- Swing time; Swing time is defined as the amount of time taken to complete one extremity of the gait cycle during the swing phase [25].
- Cadence; It's defined as the number of steps taken per unit of time [25].

- Stride time; It can be defined as the time between two successive footsteps of the same foot [25].
- Step width; step width is defined as the distance calculates between the left and right foot line of progression [25].

A schematic representation of these parameters can be seen in

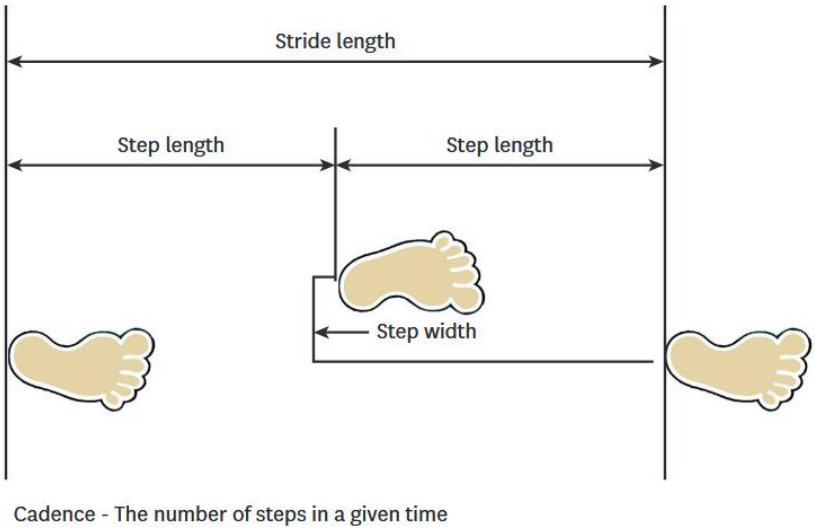


Figure 3- Schematic representation of gait parameters. Adapted from [28]

2.7 Machine Learning and Deep Learning Fundamentals

Artificial intelligence (AI), particularly Machine Learning (ML) has grown rapidly in recent years in the context of data analysis and computing, allowing the development of smart automated applications, with the ability to learn and enhance from experiences automatically without being specifically programmed [30]. The popularity of machine learning approaches has been growing day-by-day, as illustrated in Figure 4.

There are four main categories of learning algorithms: supervised, unsupervised, semi-supervised and reinforcement learning [30].

Supervised learning is typically the task of machine learning to learn a function that maps an input to an output, based on a dataset of input-output pairs. It uses labelled training data to infer the function. Supervised learning is mostly carried out when a certain set of results are identified to be accomplished from a certain set of inputs, i.e., a task driven approach. The most common examples of supervised learning include classification, that separates the data, and regression, that fits the data, such as distinguishing a number of patients affected by a determined disease from a heathy control group, for instance [30].

Unsupervised learning analysis unlabelled datasets, without the need for human interference, i.e. a data-driven approach. These techniques are widely used to extracting generative features, identifying meaningful trends and structures, groupings in results, and exploratory purposes. The most common unsupervised learning tasks are clustering, density estimation feature learning, dimensionality reduction, finding association rules, anomaly detection, etc. [30].

Semi-supervised learning can be classified as a hybridization of the above mentioned methods. Semi supervised learning uses both labelled and unlabelled data, and its main goal is to achieve a better performance than a supervised learning method, in situations where the labelled data is reduced, but the unlabelled data is numerous. Some applications of semi-supervised learning are machine translation, fraud detection, labelling data and text classification [30].

Reinforcement is a type of algorithm that enables the software to improve its efficiency, by evaluating the optimal behaviour on a particular environment, i.e., an environment driven approach. This type of method is based on penalty and reward, and its primary goal is to take environment agents into consideration to increase the reward or reduce the risk. This type of approach is useful to improve the efficiency of operational systems, but not for straightforward problem solving [30].

A schematic representation of the differences between these methods can be seen in Figure 5.

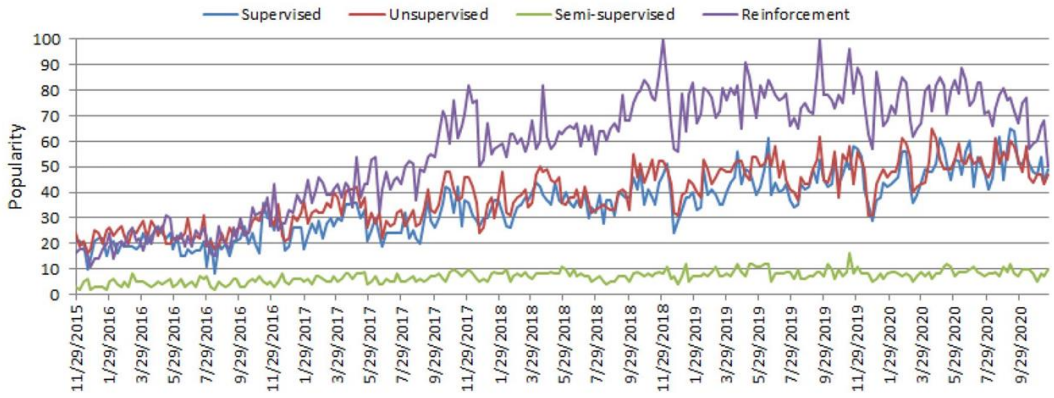


Figure 4- The worldwide popularity score of various types of ML algorithms in a range from 0 (minimum) to a 100 (maximum) from 2015 to 2020, according to Google Trends. Adapted from [30].

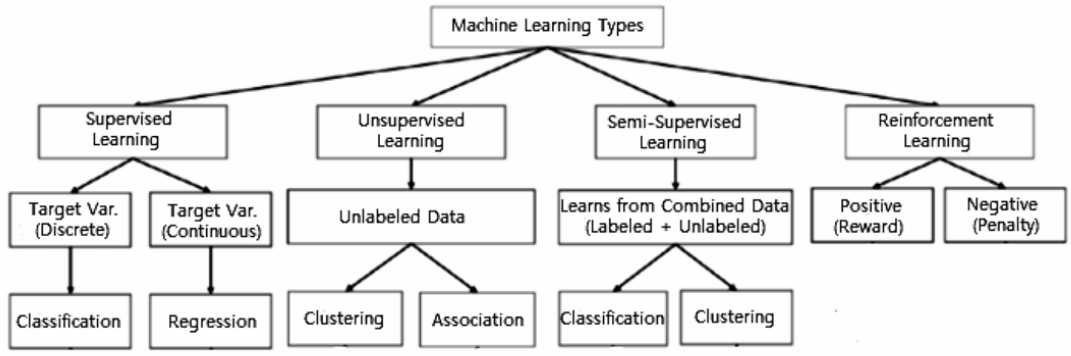


Figure 5- Schematic representation of the different ML models. Adapted from [30].

The used ML method is adapted to the performed task. There are several different ML tasks and algorithms, including classification analysis, regression analysis, data clustering, association rule learning and feature engineering for dimensionality reduction [30].

Classification analysis is regarded as a supervised learning task. It's a predictive modelling problem, where a determined label is predicted for a given example. Classification problems can, in general, be classified as binary classification, multiclass classification or multilabel classification. Binary classification refers to a classification problem with only two possible labels, such as "true or false", "yes or no". Multiclass classification refers to classification tasks having more than two classes. Given examples are classified as belonging to a class within a range of specified classes [30].

Many ML algorithms have been proposed in literature. In the following, the most commonly used ones are summarized.

- **Naïve Bayes (NB):** This algorithm is based on Bayes theorem with the assumption of independence between each pair of features. It can be used or both binary and multiclass classification. The key benefit of this method is that, when compared to other more sophisticated approaches, it requires relatively small amounts of data. However, its strong dependence on the assumption of feature independence may affect the performance. Common variants of NB classifiers include Gaussian, Multinomial, Complement, Bernoulli and Categorical [30].
- **Linear Discriminant Analysis (LDA):** This method is a linear decision boundary classifier, created by fitting class conditional densities to data and applying Bayes rule. This method projects the dataset into a lower-dimensional space, i.e., a reduction of dimensionality that minimizes the complexity of the model. The standard LDA model usually suits each class with a Gaussian density, assuming that all classes share the same covariance matrix. LDA is closely related to ANOVA and regression analysis, since it attempts to express a depend variable as a linear combination of other features [30].
- **Logistic Regression (LR):** Logistic Regression is another commonly used probabilistic based statistical model. This method uses a logistic function to estimate the probabilities, which is also refers to as sigmoid function, shown in Equation 2.1 [30].

$$f(x) = \frac{1}{1 + e^{-x}} \tag{2.1}$$

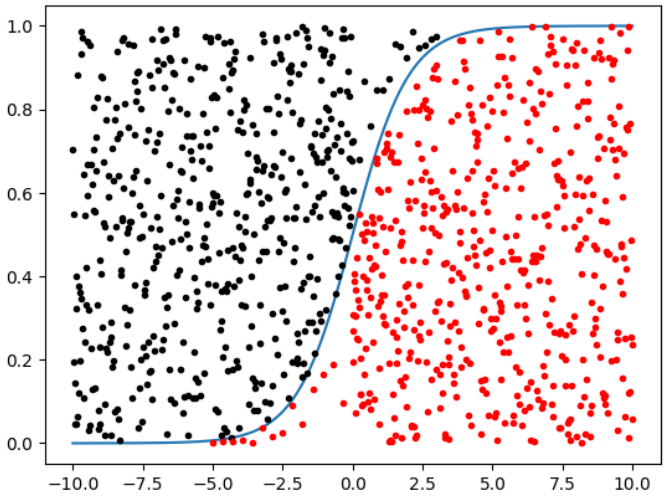


Figure 6- Schematic representation of a sigmoid decision function

- **K- nearest-neighbour (KNN):** K- Nearest- Neighbour is an instance-based learning algorithm, since it doesn't focus on constructing a general internal model, but rather stored the training data in an n-dimensional space and classifies new data points based on similarity measures. Classification is attributed based on a majority voting of the k nearest neighbours of each point. The quality of the predictions made by this model is highly dependable of the quality of the data. Regardless, KNN is quite robust to noisy data. The main issue with KNN is to choose the optimal number of neighbours to be considered. KNN can be used for both classification and regression [30]. A schematic representation may be seen in Figure 7.

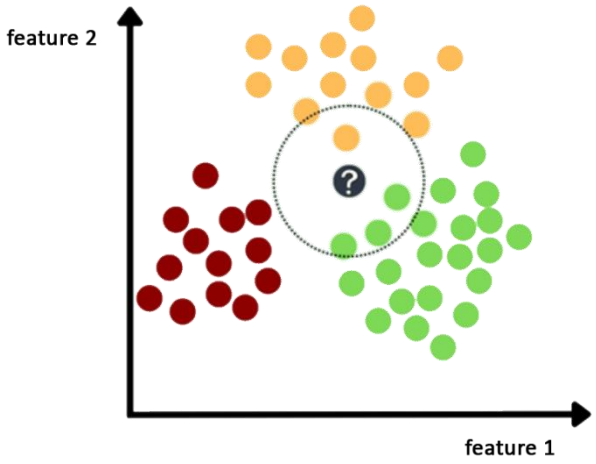


Figure 7- Schematic representation of the functioning of the K-Nearest-Neighbour algorithm. Adapted from [31]

- **Support vector Machine (SVM):** In a high or infinite dimensional space, SVM constructs a hyper-plane or a set of hyper-planes which have the greatest distance from the nearest training data points in any class. Intuitively, the hyper-plane achieves a strong separation since, in general, a greater margin brings a lower generalization error. The behaviour of the classifier is determined by mathematical functions known as the kernel. The most popular kernels used in SVM include linear, polynomial, radial basis function (RBF) and sigmoid. An optimal hyper-plane is defined as the decision function with maximum margin between the vectors of the different classes. Figure 8 illustrates an example of a 2 dimensional classification problem, with a linear kernel [30].

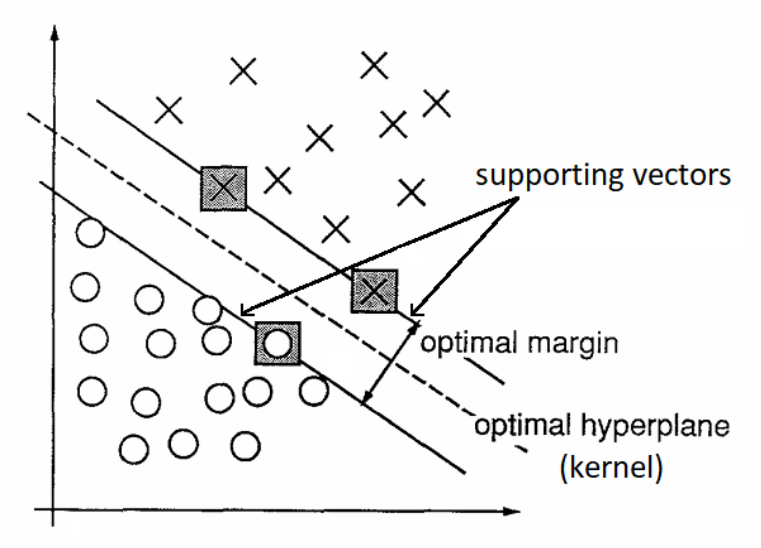


Figure 8- Example of a separable problem in a 2 dimensional space. Adapted from [30]

Decision Tree (DT): Decision Tree is non-parametric supervised learning method, used for both classification and regression tasks. Instances are classified by checking the attributes of each node of the "tree", starting in the root node of the tree and then moving down the tree branch corresponding to the attributed value. A schematic representation of this method can be found in

- Figure 9. For splitting, the most popular criteria are "gini" for Gini impurity, expressed in Equation 2.2, and entropy for the information gain, expressed in Equation 2.3 [30].

$$Gini(E) = 1 - \sum_{i=1}^{c} p_i^2 \tag{2.2}$$

$$Entropy: H(x) = -\sum_{i=1}^{c} p(x_i)\, log_2\, p(x_i) \tag{2.3}$$

- **Random Forrest (RF):** Random Forest is an ensemble classifier that fits several DT classifiers in parallel, as shown in Figure 10. These classifiers are used in parallel with several sub-sets of the dataset, and final outcome is later decided through major voting or averaging. RF model usually provides biter results than a single DT model, as the use of several decision trees reduces the overfitting problem, increasing accuracy. To build a series of decision trees with controlled variation, it combines bootstrap

aggregation (bagging) and random feature selection. RF can be used to classification and regression [30].

- **Adaptive Boosting (AdaBoost):** Adaptive Boosting is an ensemble method that employs an interactive approach to improve poor classifiers by learning from their errors. AdaBoost use sequential assembling, to build a high accuracy classifier by combining many poor performance classifiers. This model is mostly useful to improve the performance of decision trees, base estimator on binary classification problems. Although AdaBoost increases significantly the efficiency if the classifier, it can trigger overpots and is sensitive to noisy data and outliers [30].
- **Extreme gradient boosting (XGB):** Gradient Boosting is also an ensemble learning algorithm that generates a final model based on a series of individual models, usually DT. The gradient is used to minimize the loss function, similar to how neural networks use gradient descent to optimize weights. Extreme gradient boosting is a form of gradient boosting that computes the second order gradients of the loss function in order to minimize loss and advanced regularization, allowing to determine the best model taking more detailed approximations into account. XGB reduces over-fitting and is able to handle large-sized datasets as well [30].

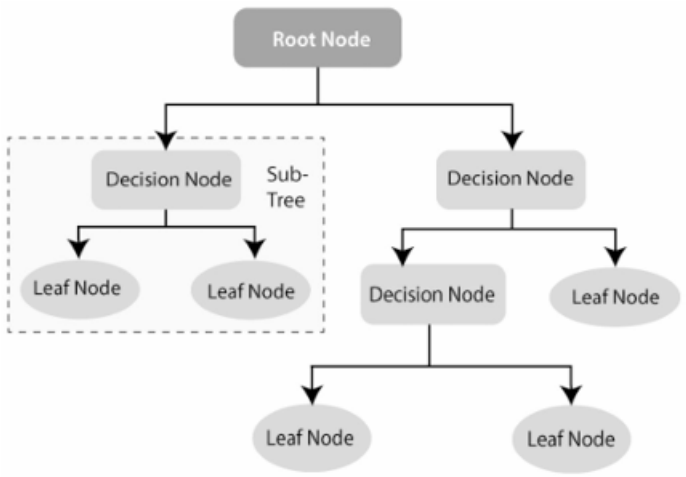


Figure 9- Decision Tree structure. Adapted from [30]

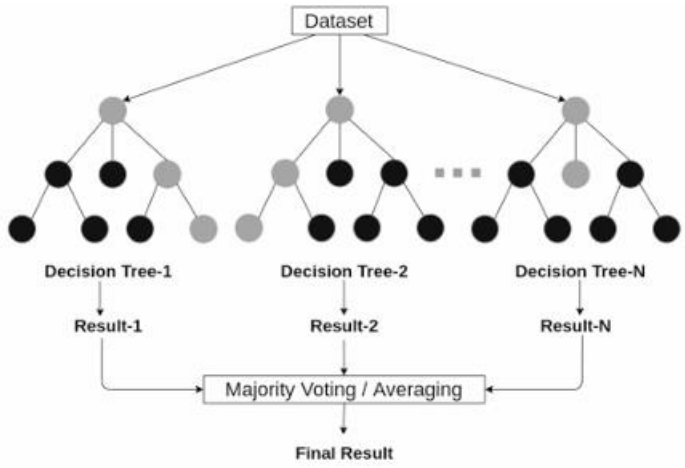


Figure 10- Example of a Random Forrest structure. Adapted from [30]

- **Categorical Boosting (CatBoost):** CatBoost is a new gradient boosting algorithm that successfully works with categorical features. This algorithm uses binary decision trees as the base predictor and uses ordered boosting, an efficient modification of gradient boosting algorithms, to overcome the problem of target leakage. Additionally, this algorithm performs random permutations to estimate leaf values when choosing the tree structure in order to overcome the overfitting. CatBoost is useful on small datasets, is able to handle categorical features and is applicable to a wide range of data types [32].

2.8 DEEP LEARNING

Deep learning is part of a wider family of artificial neural networks (ANN)-based machine learning algorithms [30]. ANNs are inspired by biological neural networks. Each ANN contains nodes (analogous to cell bodies) that communicate with the other nodes via connections (analogous to axons and dendrites) [33]. This allows the algorithm to combine several processing layers, such as input, hidden and output, to learn from the data [30]. The connections between the nodes in an ANN are weighted based on their ability to provide a desired outcome, analogously to how synapses between neurons are strengthened with correlated outputs [33]. An example of the structure of an ANN is represented in Figure 11. A simple ANN contains an input layer, a number of hidden layers between 0 and 3, and an output layer, while deep neuronal networks can have hundreds or even thousands of layers. Each layer of a ANN can have any number of nodes, although usually, the number of nodes in the output layer corresponds to the number of classes being predicted, for multi-class classification, a single node with a sigmoid activation function, for binary classification, or a linear activation function if the goal is regression [33].

The main advantage of deep learning compared to traditional machine learning is its ability to achieve better performances, particularly when trained with large datasets. Figure 12 shows the performance of DL over ML considering the amount of data [30].

As show in Figure 12, when considering small datasets the quality of the performances of ML ad DL are very close, with a slight advantage to ML. However, when considering large datasets, DL archives greater results, although this may vary depending on the data characteristics and the experiment setups.

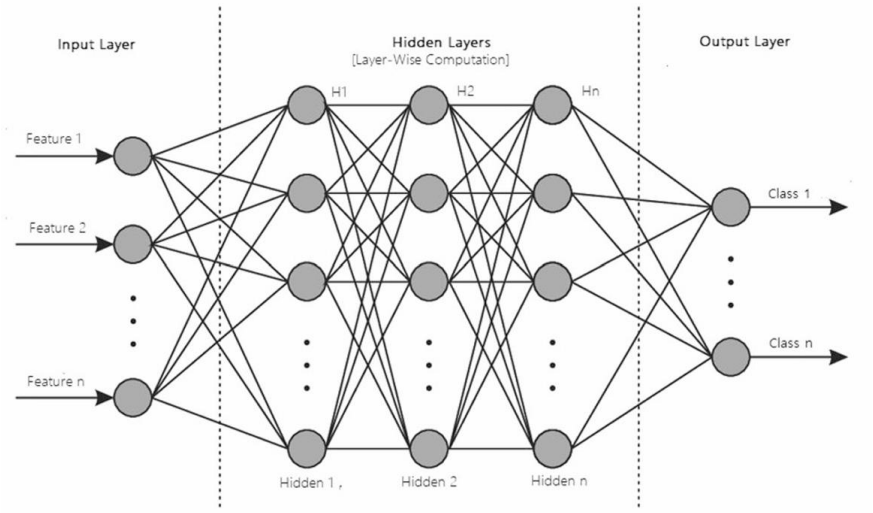


Figure 11- Representation of the structure of an ANN. Adapted from [30]



Figure 12- Performance of DL and ML in relation to the amount of data. Adapted from [30]

A summary of the most common DL models is presented below:

- **Multi-Layer Perceptron (MLP):** MLP is the base architecture of DL. The base of this algorithm, and of any artificial neural network is the perceptron. A perceptron is a machine learning algorithm that takes a series of features and their targets as inputs, and attempts to find a line, plane or hyperplane that separates the instances into classes. These features are transformed using an activation function. The most used activation function is the sigmoid function. Other popular functions include hyperbolic tangent, identity and rectified linear unit, shown in Figure 12.

A typical MLP consists of a fully connected network consisting of an input layer, one or more hidden layers, and an output layer, as shown in Figure 11. Each node in one layer connects to each node in the following layer, to a certain weight, providing information from each node in the previous layer, transformed, to each node in the subsequent layer [33].

MLP utilizes the "Backpropagation" technique to adjust the weight values internally while building the model. MLP is sensitive to scaling features and allows a variety of hyperparameters to be tuned, which can result in a high computational cost [30].

- **Convolutional Neural Networks (CNN):** A CNN is a special case of a ANN. CNNs enhance the design of the standard ANN, containing convolutional layers, pooling layers, as well as fully connected layers [30]. CNNs are often used in image processing tasks, image recognition, or image editing, since this method takes advantage of the two-dimensional (2D) structure of the input data [30]. To perform image recognition tasks with feedforward ANN, each input corresponds to a pixel, which isn't ideal because, since there aren't connections between nodes in a layer, the special relationship between pixels in an image will be lost. CNN overcomes this issue. Patches of an image are fed to specific nodes from one layer to another, instead of using single pixels as an input, preserving the spatial context from which a feature was extracted. These patches of nodes learn to extract specific features and are known as convolutional filters [33]. An example of the structure of a CNN can be found in Figure 14. Although CNN has a greater computational cost, it allows an automatic detection of the important features, without the need for manual intervention, making it more efficient than regular ANN. There are several deep learning models based on CNN used in the field, including AlexNet, Xception, Inception, Visual Geometry Gorup (VGG), ResNet, etc. [30].
- **Long Short-Term Memory (LSTM):** LSTM is an artificial recurrent neural network (RNN) architecture used in the area of DL. What distinguishes LSTM from other DL models is that, unlike regular feedforward neural networks, LSTMs have feedback links [30]. The core idea behind this is the introduction of memory cells, that can maintain their state over time, and a gating mechanism to control the flow of information. This mitigates gradient propagation issues, by ensuring a more effective gradient propagation over long sequences. A schematic representation of the architecture of a LSTM may be seen in Figure 15.

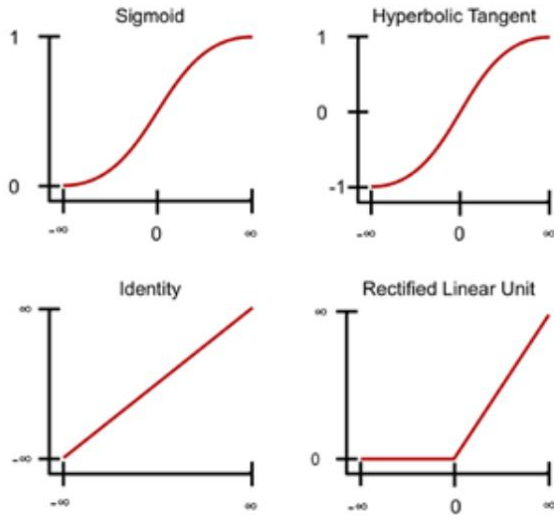


Figure 13- Examples of four different activation functions: sigmoid, hyperbolic tangent, identity, and rectified linear unit. Adapted from [33].

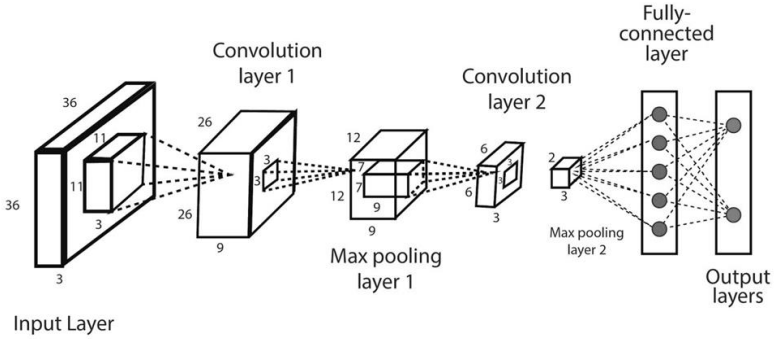


Figure 14- Example of the architecture of a CNN. Adapted from [30]

Mathematically, considering a traditional RNN, where the hidden state h_t at time step t is given by Equation 2.4:

$$h_t = tanh(W_h h_{t-1} + W_x x_t + b) \tag{2.4}$$

During backpropagation, the gradient $\frac{\partial L}{\partial h_t}$, where L is the loss function is computed. Fro long sequences, the recursive multiplication leads to whether vanishing (values close to 0) or exploding (values tending to infinity) gradients, making training unstable and inefficient. By introducing the cell state, LSTM allow gradients to flow without significant alteration. The cell state is updated according to Equation 2.5.

$$C_t = f_t \cdot C_{t-1} + i_t \cdot \tilde{C}_t \tag{2.5}$$

Where f_t, i_t and $\tilde{C}_t$ are the forget gate, input gate, and candidate cell state, respectivle. The forget gate f_t determines what fraction of the previous cell state $Ct{-}1$ should be retained, while the input gate i_t controls how much of the new candidate state $\tilde{C}_t$ should be added. This mechanism allows the LSTM to preserve the relevant information's across long sequences, while forgetting the non-relevant details [34]. LSTMs are well suited for analysing, and learning sequential data, such as classifying, processing and predicting data based on time series [30].

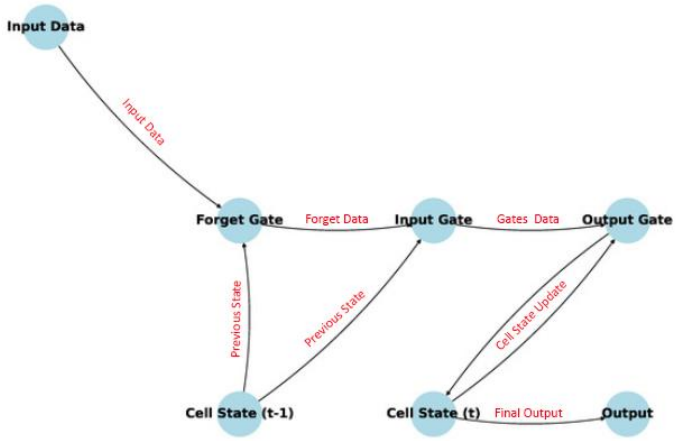


Figure 15- LSTM architecture diagram. Adapted from [34].

The attention towards DL models has been increasing in the past years, particularly in the field of medicine, given the great amount of digital availability if information however, many challenges remain present. DL is limited by the quantity and the quality of the data. In order to create a model that is both reliable and generalizable, thousands of training examples are necessary, which makes the development of identification models for rare conditions, when data might not be so easily available, all the more challenging. On the other hand, mislabelled or poor quality data has an heavy impact on the performance of the model. The risk of overfitting is also present, as a model might be overly train for the training dataset and not perform well on real-world scenarios [33].

DL models also suffer from the black box problem, meaning that an output is obtained from an input, but the process undergone by the model is not easily interpretable, and it isn't clear what features were selected or what was communicated to the model. In contrast, simple linear algorithms, although not as powerful as DL, are more easy to interpret [33].

3
SYSTEMATIC REVIEW

ML tools have revealed to be extremely useful in the support of clinical diagnosis in the last decades, and the diagnosis of PD is no exception. PD diagnosis is based on subjective clinical tests, as there are no effective biomarkers for PD, which makes it harder for clinical specialist to differentiate PD from other pathologies when symptoms overlap. Therefore, Deep Learning and Machine Learning have become more attractive in the past decade.

DL and ML models might be based on several different parameters, with gait analysis, handwriting, voice and speech, tremor and motor tasks, imaging and EEG signals among the most common. There is a high amount of developed models that based on multimodal data as well.

The most common ML algorithms used in this field include Support Vector Machine (SVM), Decision Tree (DT), Naïve Bays (NB), Logistic Regression (LR) and Random Forest (RF). Regarding DL algorithms, the most commonly used are Convolutional Neural Networks (CNN), Artificial Neural Networks (ANN), Long Short-Term Memory (LSTM) and eXtreme Gradient Boosting (XGB), among others.

A resume of the main related work in the field is presented.

This research was conducted in three different platforms: IEEE, PubMed and Scopus. The research was made with the terms Parkinson AND (diagnose OR detection) AND (ML OR DL). In order to consider only recent discoveries, only articles from 2025 and 2026 were considered. Exclusion criteria included all articles that didn't approach PD diagnosis, and articles that didn't consider biomechanical parameters. A total of 102 articles were used.

3.1 VOICE AND SPEECH

Voice and speech suffer alterations in patients with PD, mostly due to bradykinesia. The slowing of spontaneous movements leads to a decrease in the movement of facial muscles, causing speech to become more monotone and less clear, with words running together [3]. Therefore, voice and speech parameters can also be used as diagnose tools. Vocal fundamental frequency and variations of amplitude are some examples of used parameters [35].

A resume of the related work related to PD diagnosis based on vocal analysis is summed in Table 2.

Table 2- Resume of the state of the Art. Voice and Speech

Author	**Year of publish**	**Used algorithm**	**Accuracy/ Evaluation**
Das et al [35]	2025	ANN	97.13 %
Rahman et al [36]	2025	LR SVM DT RF KNN XGB Stacking Models Polynomial Features	LR: 89.74% SVM: 89.74% DT: 92.31 % RF: 94.87 % KNN: 94.87 % XGB: 94.87 % Stacking Models: 84.62% Polynomial features: 94.87%
Soltana et al [37]	2025	Bagging, Boosting, Voting, and Stacking	97%
Alrosan et al [38]	2026	SVM kNN RF LR	98.3%
Prakash et al [39]	2025	AdaBoost	97.83%
Basavaiah et al [40]	2025	RF	87%
Tougui et al [41]	2025	DL (PD-VOST)	AUC: 95.89%
Tailwal et al [42]	2025	CNN-LSTM	90%
Quamar et al [43]	2025	BiLSTM	97%
Dudek et al [44]	2025	XGB DL (Hubert)	XGBoost- F1 score 0.94 Hubert- F1-score 0.90
Nayak et al [45]	2026	SVM	95%
Kumari et al [46]	2025	CNN	Binary classification: 87.5% Multiclass classification: 93.75%
Durga et al [47]	2025	DT, RF, SVM, LR, NB, XGB Essemble model (RF +LSTM)	DT: 92% RF: 87% SVM: 82% LR: 84% NB: 69% XGB: 95% Essemble: 96%
Tekindor et al [48]	2025	AE LSTM	95.79%
Aversano et al [49]	2025	AdaBoost	98 %

Table 2- Resume of the state of the Art. Voice and Speech

Author	**Year of publish**	**Used algorithm**	**Accuracy/ Evaluation**
Qadir [50]	2025	SMOTE data augmentation Chi square feature selection XGB classification	96.4%
Mohammed et al [51]	2025	Classifier based on Clark's distance GWO for feature selection	98.3%
Pathak et al [52]	2025	RF DT KNN SVM LR	RF: 96.2% DT: 95.6% KNN: 94.6% SVM: 87.4% LR: 82.7%
Amilo et al [53]	2026	DNN	91.8%
Chakole et al [54]	2025	GB; RF; XGB; KNN; NB	GB: 94.07% RF: 90.78% XGB: 84.81% KNN: 82.83% NB: 79.83%
Singh et al [55]	2025	RF	97%
Chahar et al [56]	2025	LSTM-CNN	94.5%
Dalal et al [57]	2025	SVC; GB; XGB; Voting Classifier	SVC: 79.39% GB: 93.24% XGB: 92.74% Voting Classifier: 91.26%
Kumar et al [58]	2025	GB +LGBM +MLP	94.87%
Nimmala et al [59]	2025	FCNN	94.8%
Valarmathi et al [60]	2025	FB-DNN	96.15%
Elkharadly et al [61]	2025	Bo-FKNN	98.4%
Bashir et al [62]	2025	XGB	95%

Table 2- Resume of the state of the Art. Voice and Speech

Author	**Year of publish**	**Used algorithm**	**Accuracy/ Evaluation**
Valarmathi et al [63]	2025	LR; RF; SVM; NB	LR- AUC: 0.9 RF- AUC: 0.95 SVM- AUC: 0.92 KNN- AUC: 0.98 NB- AUC: 0.85
Athamneh et al [64]	2025	CatBoost	100%
Surya et al [65]	2025	SVM; RF; kNN	SVM: 87% RF: 79% KNN: 79%
Pradhan [66]	2025	MLP	97.43%
Shafiq et al	2026	NI-ML algorithm	93%
Dimpul Durga et al [67]	2025	LSTM-DBN	97.1%
Maheshwari et al [68]	2025	RF & Entropy & Voting Classifier	AUC: 0.98
Motamedi et al [69]	2025	Bagged essemble	VIF-BOBE-RRF VIF- RSOBE-RRF R^2 0,97 R^2 0.96 RMSE 0,04 RMSE 0.0454 MAE 0,0169 MAE 0.019
Kannan et al [70]	2025	DNN XGB SVM	97%
Abhay Karthik et al [71]	2025	XGBoost; SVM; Random Forest; and AdaBoost.	SVM: 92.3% RF: 94.8% XGB: 92.3% Voting classifier: 94.9% AdaBoost: 84.6%

3.2 DRAWING AND HANDWRITING

As a consequence of bradykinesia, hand movements become more restricted, with a decrease of the amplitude of the movements. Therefore, writing becomes cramped and small [3]. Tremors also affect hand movements, causing writing and drawing to become less clear. A resume of the related work in this matter is presented in Table 3.

Table 3- Resume of the state of the Art. Drawing and Handwriting

Author	Year of publish	Used algorithm	Accuracy/ Evaluation
Shanmugavadivu et al [72]	2025	DL	VGG19: 94.15% Xception: 97.35% InceptionV3: 96.49% EfficientNet: 9295% ResNet152: 99.8%
Nawal et al [73]	2025	CNN	99%
Mamun et al [74]	2025	ET XAI	89.27%
Aridhi et al [75]	2025	DL	91.51%
Punya et al [76]	2025	DL (Res Net VT)	96.67%
Anandapadmanabhan et al [77]	2025	DL	81%
Shastry [78]	2025	DNN	40%
Al-Jabbar et al [79]	2025	CNN	99.35%
Pareek et al [80]	2025	LR; KNN; LDA GNB; DT; SVC	LR: 72.5% LDA: 69.82% KNN: 64.28% RF: 70.71% GNB: 78.03% SVM: 48.03%
Özdemir et al [81]	2025	Vision Transformers; CNN; Elasticnet	99%
Shanthappa et al [82]	2025	CNN	99.44%

3.3 GAIT

Changes in gait are widely used as a diagnostic tool for patients with PD. With the progression of the disease, the patient manifests slowness and abnormalities in gait, including decrease of step length, less ability to turn on pivot and episodes of freezing. This method is adequate for patients who don't support more invasive methods and it provides information about the disease progression, allowing for patient monitoring.

Biomechanical gait parameters might be collected in several different ways, such as:

- Wearable sensors, i.e. sensors worn by the patient. These sensors include gyroscopes, accelerometers, or a combination of both, such as IMU (Inertial Measurement Units), that consist of electronical sensors that measure an object's angular velocity through a combination of accelerometers, gyroscopes and, sometimes, magnetometers.
- Non wearable sensors, sensors that aren't worn by the patient, such as platforms that measure the ground's reaction forces to the patient's movement.
- Images or videos, analysed afterwards by image processing methods.

Table 4- Resume of the state of the Art. Gait analysis

Author	Year of publish	Used algorithm	Accuracy/ Evaluation
Kapileswar et al [83]	2025	GNN LSTM	94%
Kumar et al [84]	2026	CNN LSTM XAI	96.7%
Pace et al [85]	2025	SVM	95%
Hemmerling et al [86]	2025	RF	81.20%
Udhayakumar et al [87]	2025	LR LDA	85%
Chen et al [88]	2026	RF	AUC: 1
Boucharas et al [89]	2025	RF; GB	RF: 84.58% GB: 87.08%
Jeba Priya et al [90]	2025	LSTM	99.1%
Ramkumar raja et al [91]	2026	ODTGMCN-NDD-SP; ET-DKF; EDT; DTGMCN	99.45%

3.4 MULTIMODAL DATA

Despite several existing methods focus on diagnosis based on one single parameter, approaches based on multimodal data are very relevant as well. The integration of multimodal data increases robustness by reducing the dependency on one single biomarker [92]. A resume of the existing work based on multimodal data is presented in Table 5.

Table 5- Resume of the state of the Art. Multimodal data

Author	Year of publish	Used data	Used algorithms	Accuracy
Ji et al [93]	2025	Multimodal gait signals	CNN-Transformer	98.81%
Mathlouthi et al [94]	2025	Multimodal data of voice signals and handwriting	DL	92.31%
Rastogi et al [95]	2025	Acoustic data (Voice, breathing, glottal noise)	EM & RF for feature selection CNN for classification (RMS, RAE, RSE)	RMS: 99.6% RAE: 55.21% RSE: 58.12%
Aggarwal et al [96]	2025	Multimodal data (biological, clinical and imaging)	Multi-Layer-Stacking	97.38%
Kumar et al [97]	2025	Multimodal data from EEG signals and handwritten tasks	BLSTM (Bidirectional LSTM) GWO optimization	99.3%
Singh et al [98]	2026	Multimodal data (hand tremors and clinical data)	Voting Classifier	99.48%
Shanthini et al [99]	2025	Multimodal data based in voice sgnals and hand-drawn images	CTSO-ZFNet (DL)	89.69%
Kukreja et al [100]	2025	Multimodal data from MRI, dopamine transporter scan and clinical biomarker	STFP GNN TCN	AUC-PR- 0.94
Chowdhury et al [101]	2025	Multimodal data based on PET image and tremor detection	Hough Transform; XGB	95.42%
Ivanova et al [102]	2025	Multimodal data from motor tasks, extracted with wereable sensors and cameras	Light GBM	Precision: 98,6 Recall: 98,1 F1-score: 98,3

Table 5- Resume of the state of the Art. Multimodal data

Author	**Year of publish**	**Used data**	**Used algorithms**	**Accuracy/ Evaluation**
Chakraborty et al [103]	2025	Data from EEG signals, MRI images and images of spiral and wave drawings	LR, VGG	VGG-spiral: 97,7%. LR-EEG: 95,74%. VGG- MRI: 96,78%
Keerthana Devi et al [104]	2025	Drawing and speech tasks	FNN	96%
Reddy et al [105]	2025	Voice, imaging data, genetic information and clinical evaluations	AEO-DBN	98.29%
Hammoud et al [106]	2026	Motor tasks signals, collected with a left-wrist-worn sensor	DL (VGG16, InceptionV3, MobileNetV2, ResNet50V2)	PD vs HC: F1 score- 0,986 PD severity: F1 score- 0,878
Singh et al [107]	2025	Motion and vocal data, based on motor tasks	MLP	95%
Esan et al [108]	2025	Demographic, medical history, lifestyle, clinical symptoms, cognitive, and functional assessments	SVM; KNN; LR; RF; XGB	KNN: 79% SVM: 84% LR: 83% XGB: 92% Stacked ensemble: 92% RF: 93%
Sahana et al [109]	2026	Voice and handwriting data	RF; CNN	SVM: 92.3% RF: 94.87% XGB: 92.3% AdaBoost: 84.6% Hybrid: 94.9%

3.5 OTHERS

Besides the already mentioned parameters, there are other symptoms, both motor and non-motor, that can be explored as diagnosis tools, including facial expressions, grip force tasks and EMG signals, among others. A resume of the related work found on this topic can be seen in Table 6.

Table 6- Resume of the state of the Art. Other symptoms

Author	Year of publish	Used data	Used algorithms	Accuracy/ Evaluation
Al-Amin et al [110]	2025	Clinical data	KNN	98.31%
Nagaraju et al [111]	2025	EMG signals	DL	99.8%
Lopez et al [112]	2025	Patient's demographic and biomarker data	RF	94%
Hathaliya et al [113]	2026	Tremor data accessed with acelerometers	GRU LSTM	74.1%
Wu et al [114]	2026	Videos of patient's facial expressions	RF	82.4%
Neto et al [115]	2025	Grip force tasks	DNN	91%-95%
Mahali et al [116]	2025	multi-sensor movement data during dynamic motor tasks	Transformer	100%

3.6 STATISTICAL ANALYSIS

Regarding ML models based on only one symptom, voice and speech is the most commonly used, followed by handwriting and drawing, EEG signals and gait analysis. Models based on multimodal data correspond to 18 % of the articles found, with the majority of the models based on voice, handwriting and imaging data. A schematic representation of the most used parameters and algorithms is presented in Figure 16 and

Figure 17. A representation of the most used parameters in models based on multimodal data can be seen as well, in Figure 18.

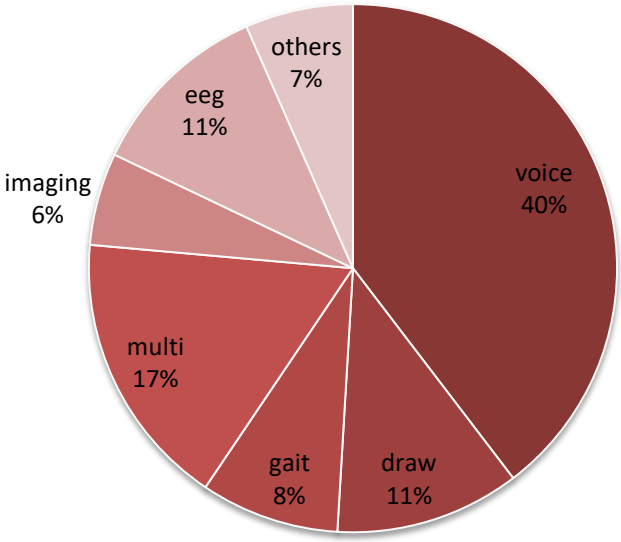


Figure 16- Schematic representation of the most used parameters in the development of ML and DL models for PD diagnose

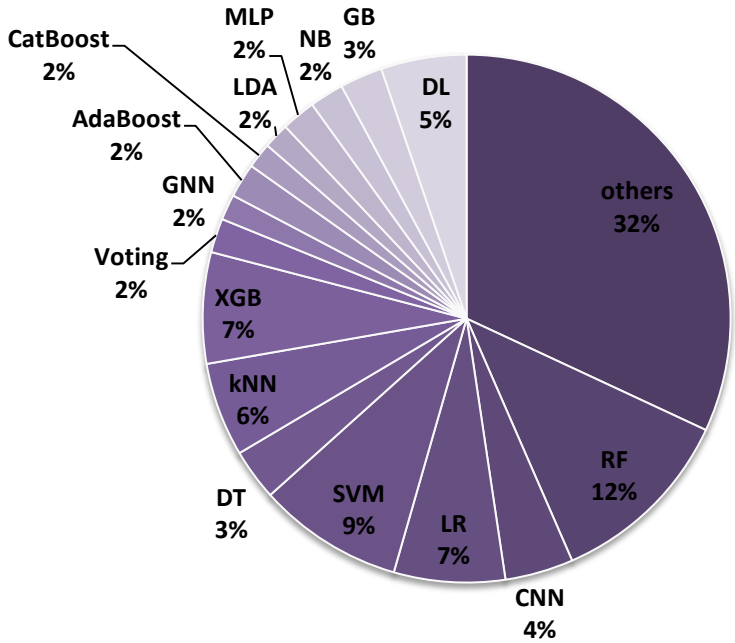


Figure 17- Schematic representation of the most used algorithms in the development of ML and DL models for PD diagnose

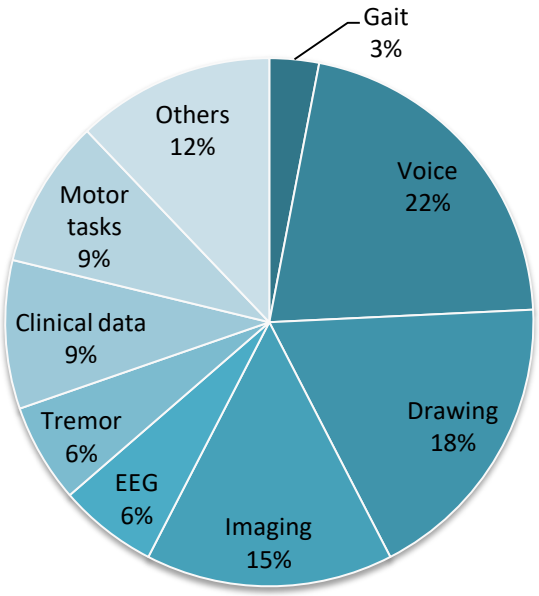


Figure 18-Schematic representation of the most used parameters in the development of multi data-based models for PD diagnose

4
DATA PREPROCESSING

4.1 DATA AUGMENTATION

The dataset is the input of the ML and DL model. The dataset is the factor that has the biggest impact on the performance of the model, so it's of major importance to have a wide and complete dataset, with quality data. To ensure good performance, ML and DL techniques require large amounts of quality data. However, in many real world applications it is not feasible to obtain sufficient training data. The main objective of data augmentation techniques is to increase the volume, quality and diversity of the training data. For a given dataset, data augmentation operated by composing a series of transformations that might be applied to the original dataset to create additional training data without altering the corresponding labels [117]. The most reliable data augmentation method to use on a determined dataset varies depending on the quality of the data.

The data used in this study were numeric spatiotemporal gait parameters, ergo, tabular data. The most used data augmentation techniques for tabular data include:

- Adding noise (Jittering). This is one of the most basic data augmentation procedures. It works by adding small random noise to the numerical features to create variations [118].
- Feature permutation. This method consists on swapping values in the same column while maintaining the distribution [118].
- Synthetic data with mean and standard deviation. This technique creates new samples, based on the mean and standard deviation of the existing data [118].
- Categorical Feature Augmentation. This technique focus on the augmentation of categorical data, by shuffling generating new values based on frequency [118].

Data augmentation is also used to solve class imbalance, when the available data for one class is disproportional in quantity compared with other the data from another class, in classification problems. The most commonly used method in literature to solve class imbalance is Synthetic Minority Over-sampling Technique (SMOTE).

SMOTE generates samples from the minority class by using the k-nearest neighbours method [118]. This allows the generation of new synthetic data based on extrapolations of existing data, which creates a consistent new dataset. This allows the addressing of under sampled data in a more efficient way than creating duplicates of the existing data [119].

Data augmentation techniques are also important to handle missing values. When a dataset contains missing data, simply discharging the instances with missing values would decrease the available data and, therefore, affect the performance of the model. On the other hand, imputing the missing values would be difficult and time consuming. Data augmentation methods mange to generate synthetic data, to replace the missing values, and increases the availability of the dataset. Generative Adversial Networks (GAN) are a commonly used method, that creates realistic synthetic data, and manages to generate categorical and continuous variables while preserving dependencies [118].

GAN algorithms comprise 2 neural networks trained using an adversarial process, in which one model- the "generator"- generates synthetic data while the other- the discriminator- distinguishes between real and synthetic data. Conditional Tabular Generative adversarial Network (CTGAN) is a type of GAN design specifically to generate synthetic data from tabular data [120]. An illustration for a CTGAN model is shown in Figure 19

.

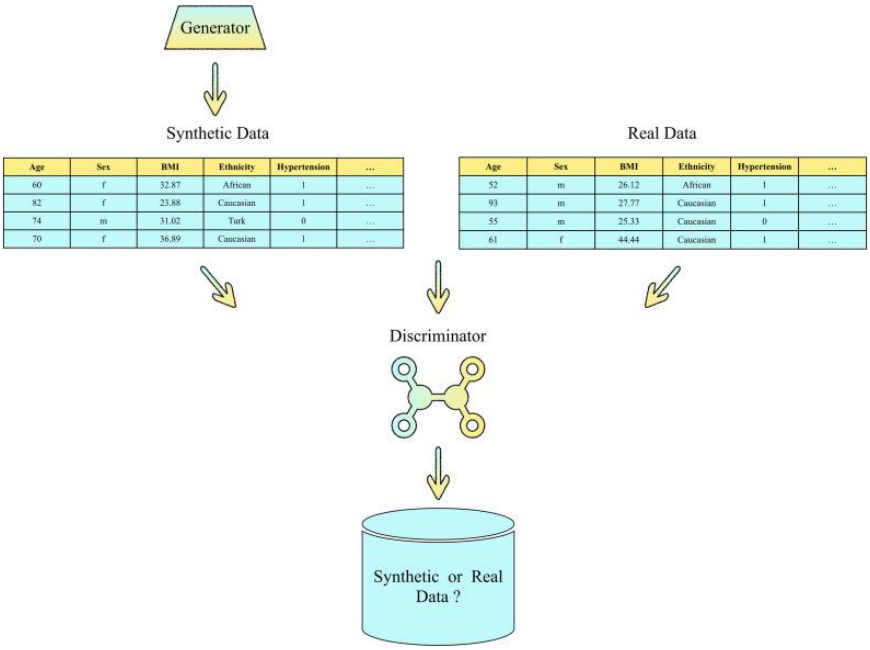


Figure 19- Illustration of a CTGAN model. Adapted from [40]

4.2 NORMALIZATION

Data normalization is a process that aims to transforms the values if the dataset into the same scale. Data normalization is particularly important in the analysis of data with high variability, where parameters are rated in different scales. When values lie on the same numerical scale, they are considered with the same importance, which provides better results. There are three normalization techniques: Z-score, Min-Max Normalization and normalization by decimal scaling [121].

- Z-core normalization is a statistic method that transforms the data, so it has an average of 0 and a standard deviation of 1. This allows for the comparison between data that lie on different scales. The Z-score normalization can be formulated as Equation 4.6 [121].
- Min-Max normalization is a statistic method that rescales the data so it fits into a specific range (usually between 0 and 1). The minimum value of the dataset is assigned to 0, and the maximum value is assigned to 1. The other values are assigned proportionally, according to Equation 4.7 [122].
- Normalization by decimal scaling is a technique that normalizes attribute values by shifting the decimal point. This scales the values between a common range strictly between -1 and 1, while preserving their relative differences and proportions. Each data value v is divided by 10^j, where j is the **smallest integer** such that the maximum

absolute value of all normalized data points remains less than 1, according to Equation 4.8 [121].

$$Z_{score} = \frac{X - \mu}{\sigma} \tag{4.6}$$

$$x_{scaled} = \frac{x - min(X)}{max(X) - min(X)} \tag{4.7}$$

$$v' = \frac{v}{10^j} \tag{4.8}$$

4.3 EVALUATION METRICS

In order to evaluate the performance of the different algorithms, and be able to discriminate which achieved the better results, is necessary to have adequate evaluation metrics, that provide information of the algorithm's performance. The most commonly used evaluation metrics o ML and DL models include:

- Confusion matrix. This is the base of all the metrics. The confusion matrix unites the four main measurements of the algorithm's performance when compared to the ground truth: True Positive (TP), i.e., correctly identified positive values; True Negative(TN), i.e., correctly identified negative values; False positive (FP), i.e. negative values incorrectly identified as positive; and False Negatives (FN), i.e., positive values incorrectly identified as negative [123].
- Accuracy (Acc): it's a measurement of the proportion of correctly identified values. The main problem of this measurement is that it might be deceiving in imbalanced datasets. It's determined according to Equation 4.9 [123].

$$ACC = \frac{TP + TN}{TP + TN + FP + FN} \tag{4.9}$$

- Recall (Rec): Measures the ability to correctly identify positives. It's determined according to Equation 4.10 [123].

$$\frac{TP}{TP + FN} \tag{4.10}$$

- Precision: Measures the proportion of predicted positives that are actually positive. It's determined according to Equation 4.11 [123].

$$\frac{TP}{TP + FP} \tag{4.11}$$

- F1-score: It's the harmonic average between precision and recall. It penalizes unbalances between FP and FN. It's calculated according to Equation 4.12 [123].

$$F1 = \frac{2TP}{2TP + FP + FN} \tag{4.12}$$

4.4 FEATURE ENGINEERING

Feature engineering is a set of actions devoted to the preparation of raw data, to be used by algorithms of automated analysis [124]. The steps in feature engineering processes are:

- Exploratory data analysis and data preprocessing. The main goal of this step is understanding the quality and quantity of the adat vailabl and preparing it for further use [124].
- Feature extraction. The objective of this step is cinverting the available data into descriptive features [124].
- Feature reduction or selection. Determine the most valuable feature for further use, by either selecting the useful features, or by reducing the dimensionality of the feature vecoe, in order to keep only the useful features [124].

There are several different techiques used to perform feature engineering, including:

- Partcle Swarm Optimization (PSO). PSO is a well-known metaheuristic algorithm used in real-world optimization problems. It's based on the behaviour of multiple natural systems, in which elements (animals) group, either to protect themselves or to hunt together. This algorithm operates in the concepts of a swarm (a group of particles), which in this framework, is understood as a collection of candidatre solution for the considered problem. Each candidate solution represets the behavirou of n individulas, eho progress through the search space. This progression is driven by the information each individual gathers about itsef and about the group. The goal of the swarm is to obtain a solution that fits the stopping criteria, through multipole iterations within the search space, whose limits are specified in the optimization problem [125]. The structure of this algorithm can be observed in Figure 20.

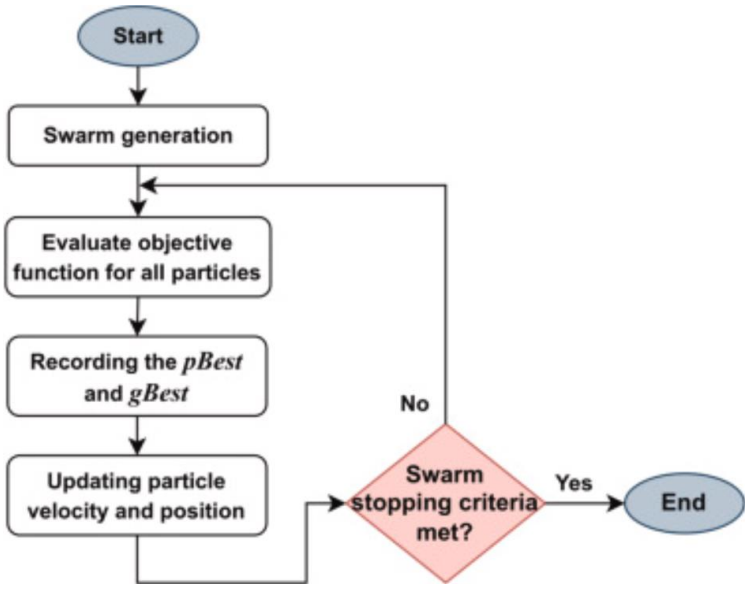


Figure 20- Structure of the PSO algorithm. Adapted from [125]

- Slime Mould Algorithm (SMA). SMA is a population based metaheuristic algorithm used in optimization problems. SMA takes the form of the Slime Mould Physarum polycephalum, a complex amoeboid structure, while searching for food [126]. It can be divided in two main types of updating. The first type involves an extensive global search within a given space, guided by the best individual, combined with random step oscillations. The second tye involves a localized search around the optimal individual, focusinf on fine-tuning and refining its own search. SMA has demonstrated outstanding performances and robustenessin several scenarios, but it still presents some limitations, such as a tendency to converge to local optima, which deacreses accuracy [127]. The SMA procedure can be visualized in Figure 21.

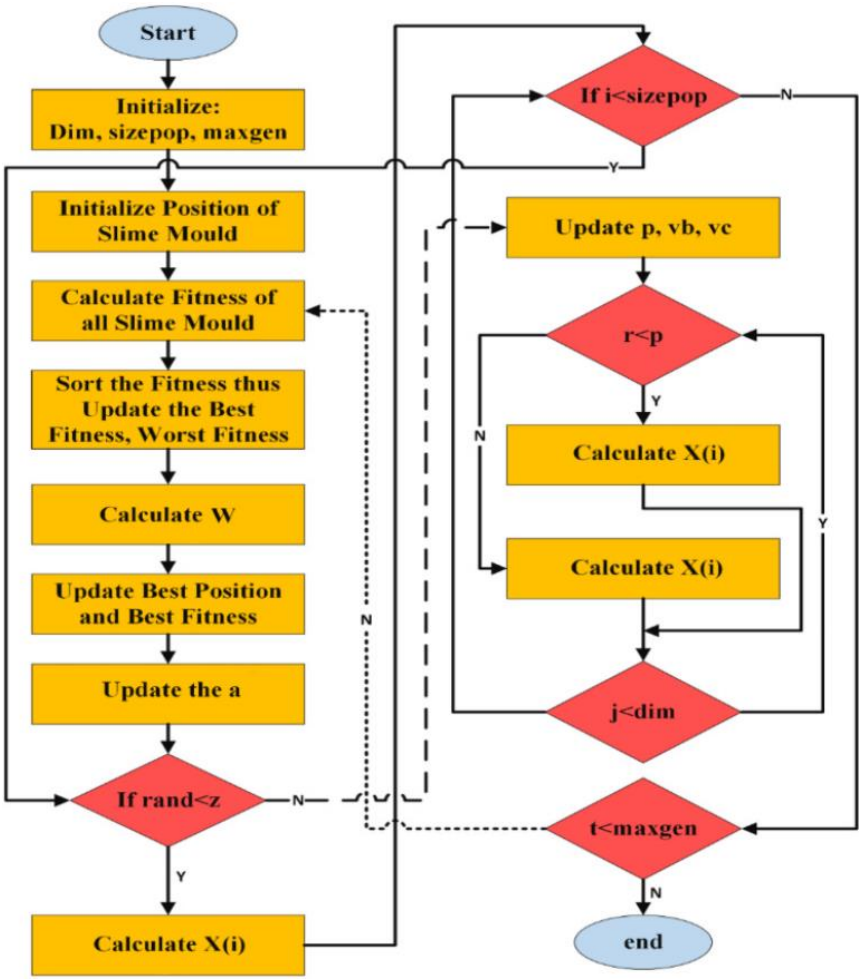


Figure 21- Clear and thorough SMA procedure. Adapted from [126]

- Whale Optimization Algortihm (WOA). The WOA algorithm mimics the behaviour of humpback whales. When huntng in group, the humpback whales can recognize the location of the prey and encircle it. In a similar way, the position of the optimal solution of an optimization problem in the search space isn't known a priori, so the WOA algorithm assumes that the current best candidate solution is the target prey, or is close to the optimum. The WOA algorithm starts with a set of random solutions. At each iteration, search agents update their positons with respect to either a randomly chosen search agen or the best solution found so far. The WOA algorithm is terminated when a termination criteria is satisfied [128].

5
METHODOLOGY

This chapter outlines the methodological framework conducted in this study.

5.1 DATASET

The data used in this study was collected at the posture and Gait Studies Laboratory of São Paulo state University, in Brazil.

The dataset contains data from 193 individuals, divided in two groups: patients diagnosed with PD, which contains 130 participants, from which 68 are men, 59 are women, and 3 are unidentified, neurologically heathy control group, containing 62 individuals, from which 31 are men and 31 are women. All the participants completed a Free walking test (FrW), while subsets of the sample also performed additional walking tasks, including dual-task walking (DTW), obstacle walking (OBW), and fast walking (FaW). Dual tasking was performed by 99 patients and 41 individuals from the control group, Obstacle Walking was performed by 98 patients and 62 healthy controls, and Fast Walking was performed by 103 patients and 20 healthy control. PD patients had a confirmed diagnosis according to the UK Parkinson's Disease Society Brain Bank clinical criteria. Disease severity was between mild and moderate range, on H&Y stages I-III. Clinical evaluations included the H&Y scale, the MDS-UPDRS scale; specifically part III, regarding motor evaluation, and the Mini-Mental State Examination (MMSE). Individuals with MMSE scores above 24 were not considered for this study, in order to ensure the absence of significate cognitive impairment. The exclusion criteria of the participants in this study included any neurological, muscoskeleton or sensory disorders that could have an impact on gait, including dementia, vestibular dysfunction or orthopaedic conditions. All PD participants were on regular medication and were accessed in the optimally medicated "on" state.

The healthy control (HC) were free of any neurological disease, and able to ambulate the room unassisted, without the need of any medical devices, and matched the PD group on age and sex distribution. Each study received approval from the institutional research ethics committee, and all participants provided informed consent before data collection.

The clinical and demographic characteristics of the participants in both groups are summed in Table 7.

Table 7- Demographic parameters of the PD patients and the HC group.

Parameter	**PD patients Mean +- std**	**HC Mean+-std**	**P**
Gender	31M/31F	68M/58F/4U	
Age(years)	64.77±8.57	68.70±8.95	0.004*
Weight(Kg)	76.41±15.53	72.83±13.38	0.124
Height(cm)	163.66±8.50	159.96±22.55	0.107
MMSE(points)	28.16±1.50	26.72±3.48	<0.001*
HAS Anxiety(points)	7.51±4.17	6.42±3.72	0.132
HADS Depression(points)	4.74±2.51	6.66±3.97	<0.001*

*Indicates values that have a statistically significant difference (P<0.05)

The demographic and clinical distributions are further illustrated in

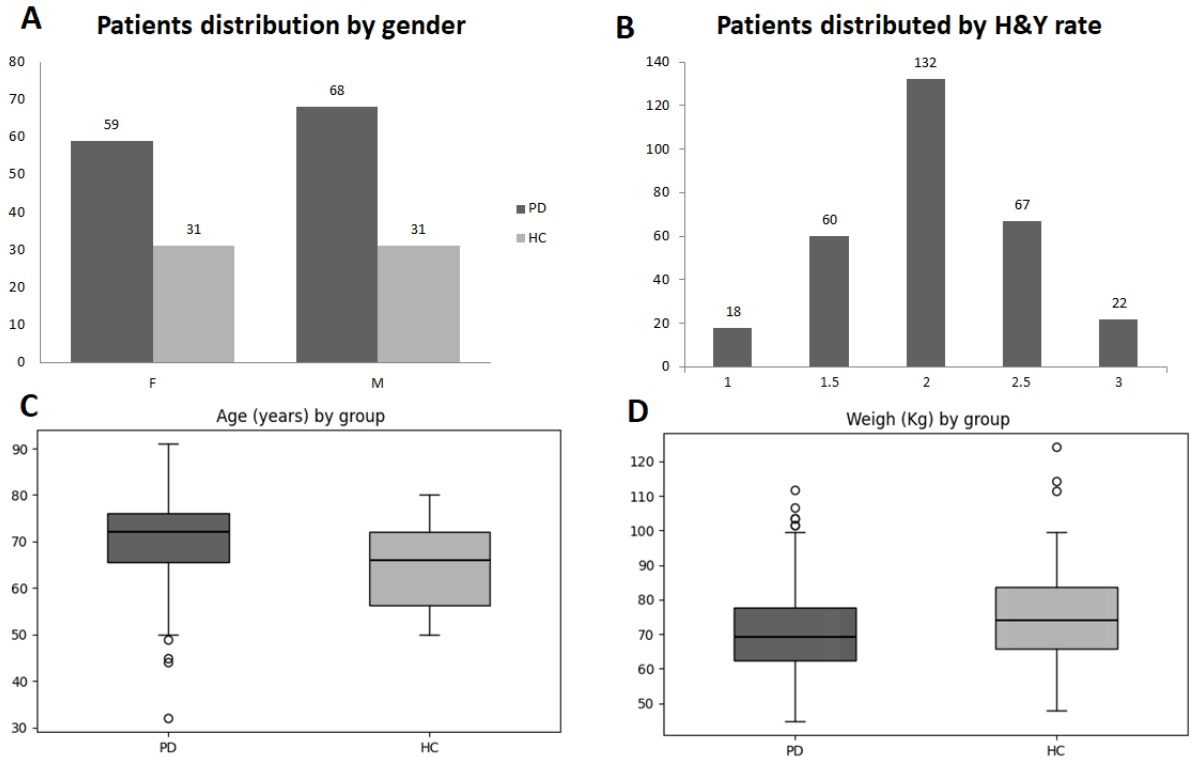


Figure 22 and Figure 23.

In general, the PD and HC groups are comparable regarding anthropomorphic characteristics, such as weight, high and age, with no significate differences between them. Regarding demographic composition, there's a balanced composition of men and women on both groups as well. The dimension of the PD group compared to the HC group however is disproportional, as the PD group has a much bigger number of participants.

Within the PD group, most patients were classified between early to moderate stages, with H&Y scores between 1.5-2.0.

PD patients also exhibited lower MMSE scores compared with the control group, as well as higher depression levels, according to the Hospital Anxiety and Depression Scale. (HADS), although the anxiety levels exhibited wide variability. The age distribution indicates that PD patients tend to be older than the control group, which confirms that the dataset represents a typical chort of older adults with mild to moderate PD and aged matched healthy controls.

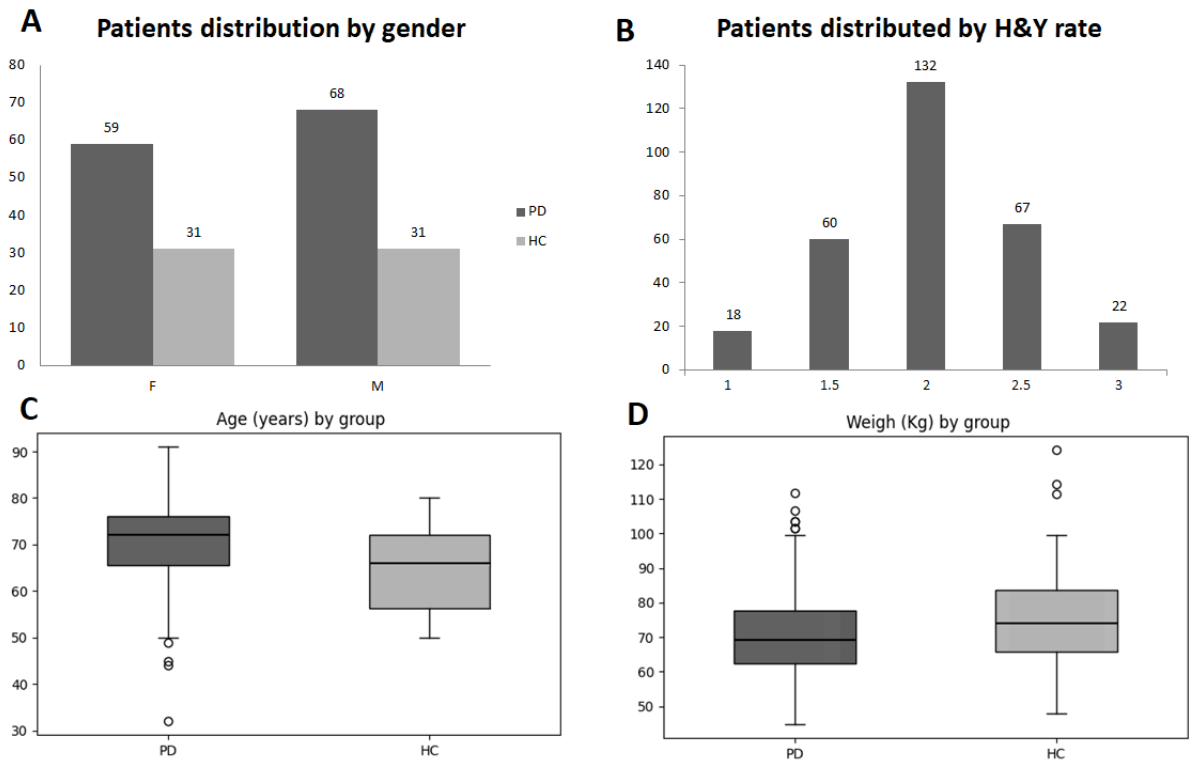


Figure 22- A) Distribution of participants by sex (female, F; male, M). B) distribution of PD patients by H&Y stage. C) Distribution of participants by age, across groups. D) Distribution of participants by weigh across groups.

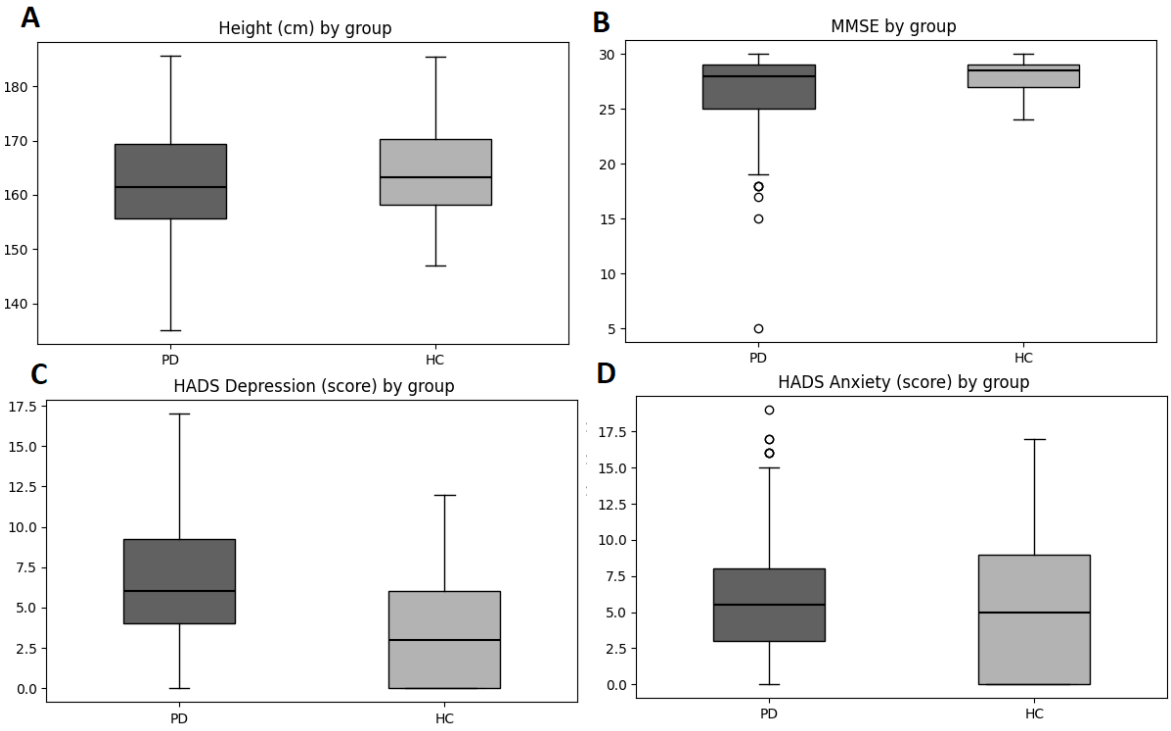


Figure 23- A) distribution of participants by height (cm) across groups. B) Distribution of participants by MMSA score across groups. C) Distribution of participants by HADS Depression score across groups. D) Distribution of participants by HADS Anxiety score across groups

5.2 GAIT TASKS

To evaluate gait performance of different individuals from both groups, several gait tasks were performed, where participants whether walked on a clear path, avoided obstacles, or attempted to perform different tasks simultaneously.

5.2.1 Free Walking

This task was performed by all the participants. In this task, participants were instructed to walk in a straight line at a self-selected comfortable pace, without restrictions or obstacles. Each subject completed at least three trials, at a wide walkway with 8.0m length and 1m width.

Data were collected using either the GAITRite electronic walkway (200 Hz), or the Optotrak Certus motion capture system (100 Hz), which tracked infrared markers attached to the forefoot and heel of each shoe.

5.2.2 Dual Task Walking

Participants who performed the Dual Task walking were asked to count either the odds or even digits, between 1 and 9, presented randomly through a loud speaker, while along an 8 meter circuit. At the end of each trial, participants reported the total count. Participants were instructed to whether do FrW only, or do DTW randomly, so the participant wouldn't anticipate which trials would involve the cognitive task. Each patient performed five DTW trials, and gait data were recorded using the GAITRite walkway (200 Hz), connected to a computer running GAITRite software for data storage and processing. In some trials, pre cortal activity was also measured with a portable fNIRS system synchronised with gait events, simultaneously, in order to enable cortical activity analysis as well.

5.2.3 Obstacle Walking (OBW)

Participants who perform OAW were instructed to walk the same 8 meter walk-way, but with an obstacle placed in the middle that they had to step over. The obstacle was standardized to 50% of the participant's knee high, 60 cm width and 3 cm depth. Each subject completed six trials, alternating the leading limb, granting an equal number for trial for left and right leg. The participant had to adapt step length and elevation to step over the obstacle without contact. Data were captured with the Optotrak Certus optoelectronic system (100

Hz), positioned in the sagittal plane. Four active markers were attached to the 5th metatarsal and lateral calcaneus of the right foot, and the 1st metatarsal and medial calcaneus of the left foot. An additional marker was fixed to the obstacle edge to measure clearance.

5.2.4 Fast Walking

The participants who performed Fast Walking were instructed to walk as fast as they could at the same 8 meter walk-way, but still at a safe pace that did not require running. This allows for an examination of gait characteristics at its maximum effort. This task was always performed with appropriate safety precautions and the required rest between trials. Gait was measured with the GAITRite (5.74m, 200 Hz).

5.3 DATA PRE-PROCESSING AND EXTRACTED PARAMETERS

The data extracted from GAITRite doesn't require additional filtering, as the system computes gait parameters directly from footfall activation patterns. All systems were calibrated before each session, to minimize systematic errors related to calibration mistakes. The instrumental provided high temporal resolution (5-10 ms) and spatial accuracy (≈ 1 cm), enabling the detection of subtle gait changes. Participants wore their regular footwear, performed practice trials when necessary, and were given rest between trials to minimise fatigue.

A comprehensive set of spatiotemporal parameters was obtained from raw recordings including mean, standard deviation and asymmetry of the step length, step time, step velocity, step width and double support time. These measurements provided detailed information about gait stability, performance and asymmetry. Asymmetry was obtained using the asymmetry index, according to Equation 5.13, which compares the most affected to the least affected side in PD, or dominant to non-dominant limb in control.

$$Assymetry\ Index = \frac{\left|X_{least\ affected\ side/\ dominant\ limb} - X_{most\ affected\ side/\ non-dominant\ limb}\right|}{X_{least\ affected\ side/\ dominant\ limb} + X_{most\ affected\ side/\ non-dominant\ limb}} \times 100 \quad (5.13)$$

To compare the values of each spatiotemporal parameter between PD and HC groups, three different feature selection methods were used: PMO, SMA and WOA. These were implemented with the Wrapper feature selection toolbox in Matlab. Each method was applied to the data regarding each of the performed walking tasks, with three attempts each. The selected features were the ones that obtained the highest accuracy. The results may be seen in Table 8, Table 9 and Table 10.

Table 8- Feature selection with PSO

Walking Task	Accuracy	Features
FrW	79.37%	Step length mean Step time asymmetry Step time standard deviation Step velocity mean Step velocity Standard deviation
DTW	100%	Step length mean
OBW	93.02%	Step length standard deviation Step velocity mean Step velocity standard deviation Step width mean Step width asymmetry Step width standard deviation
FaW	95%	Step length mean Step length asymmetry Step length standard deviation Step time standard deviation Step velocity asymmetry Step velocity standard deviation Step width mean Step width asymmetry ds standard deviation

Table 9- Feature selection with SMA

Walking Task	Accuracy	Features
FrW	90.48%	step length standard deviation Step velocity asymmetry Step width asymmetry Step width standard deviation
DTW	100%	Step width standard deviation
OAW	93.02%	Step time standard deviation Double support standard deviation
FaW	97.5%	step length mean Step velocity mean Step velocity asymmetry Step velocity standard deviation

Table 10- Feature Selection with WOA

Walking Task	Accuracy	Features
FrW	93.65%	step length mean step length standard deviation Step time standard deviation Step velocity asymmetry Step velocity standard deviation Step width mean Step width asymmetry Step width standard deviation Double support mean
DTW	100%	Step length mean
OAW	90.7%	Step time standard deviation Double support mean
FaW	100%	step length mean Step time standard deviation Step width asymmetry Step width standard deviation Double support standard deviation

5.4 EXPERIMENTAL SETUP

This section contains a detailed description of the workflow followed in this thesis.

The process began with data analysis and preparation, followed by the division of the dataset into two subsets: an independent test set comprising 20% of the data, and a training set comprising 80% of the data.

Several participants had missing parameters, causing "blanc spots", which highly reduced the available data for the training of the model. Therefore, Conditional Tabular Generative Adversarial Network (CTGAN) was used to generate new data based on the available data, in order to fill the missing parameters when required. Afterwards, the data was normalized using the Minimax scale normalization.

ML and DL classifiers were then trained on the pre-processed training folds and evaluated on the corresponding validation folds. Class imbalance was addressed using Synthetic Minority Over-sampling Technique (SMOTE) algorithm, in order to balance the disproportion between he participants in PD and HC groups. The model performance was addressed through four metric evaluations: accuracy, f1-score, recall and precision.

The implementation of the methodology was supported by a set of python libraries that provided the necessary tools.

For numerical and scientific computing, the numpy library was used, for operations regarding vectors and matrices. Additionally, the pandas library was used to read and store information form excel files.

The pandas library was used to read and store information from excel files. The CTGAN algorithm was implemented using the svd.ctgan library, while SMOTE was applied recurring to the imblearn.over_sampling library. The ML algorithms were implemented primarily with the scikit-learn library, with the exception of the XGBoost algorithm, that was implemented with the xgboost library. The scikit-learn library was also used to implement the minimax scale. To perform the evaluation of the model, the scikit-learn.metrics library was used to compute the accuracy, f1-score, recall and precision. Finally, for visualization, matplotlib.pyplot was used.

5.4.1 Data preparation and splitting

The dataset used in this work was originally stored in four separate Microsoft Excel files, two for the records of patients with PD and two for the records of the HC group. For each pair of excel files, one contained the demographic information, while the other contained four spreadsheets corresponding to the spatiotemporal gait parameters for the four walking tasks.

An initial inspection revealed certain inconsistencies in feature naming between the PD and the HC files, such as sw_mean and step_width_mean, both representing step width mean. To ensure uniformity across groups, all features were standardised to a consistent naming convention.

The data from the excel files was later structure into DataFrames using the pandas library, where each row represented one participant record and each column represented a gait parameter. The participant record was identified by an unique code and, for PD patients, also the year of collection. A label binary label was also added to each row, where 1 corresponds to a PD patient and 0 corresponds to HC. This procedure was repeated separately for each walking task, resulting in one DataFrame per task.

5.4.2 Data pre-processing

The gait data contained exclusively numeric spatiotemporal parameters, but some patients had missing values in specific parameters, and there was a difference in scale across features, which makes the pre-processing of data a crucial step. To avoid discarding valuable data, CTGAN was applied to each missing value, in order to complete the dataset with valid values in the missing feature.

Since gait parameters operate in different scales, all features were rescaled to the range [0,1], with min-max normalization.

5.4.3 Feature Engeneering

Although all features may have clinical relevance, not all contribute to perform a distinction between PD patients and HC. Furthermore, including highly redundant variables can increase dimensionality unnecessarily and reduce classifier performance. To address this, feature selection was performed, recurring to the wrapper feature selection toolbox in matlab.

This toolbox used three different methods to performed feature selection: Particle Swarm Optimization (PSO), Slime Mould Algorithm (SMA), and Whale Optimization Algorithm (WOA).

Each method was performed three times, and the features were selected based on the highest accuracy achieved.

5.4.4 Classifier Implementation

A diverse set of ML and DL classifiers was explored, ranging from traditional statistical models to modern NN. While the theoretical foundations of theses modes were previously described, this section described their practical implementation. The hyperparameters used were obtained based on the default parameters described in python documentation.

5.4.4.1 Support Vector Machine (SVM)

The SVM classifier was implemented using scikit learn's SVC class. The hyperparametrs of this classifier are shown in Table 11. These were based on documented values [129].

Table 11- Hyperparameters of the SVC classifier

C	1
kernel	rbf
degree	3
gamma	scale
coef0	0
shrinking	True
probability	False
tol	0,001
cache_size	200
class_weight	None
verbose	False
max_iter	-1
decision_function_shape	ovr
break_ties	False
random_state	None

5.4.4.2 K-nearest neighbour (KNN)

k-NN was implemented using scikit-learn's KNeighborsClassifier. The key hyper parameters for k-NN included the number of neighbours k, the distance metric, such as Euclidean, Manhattan, or Minkowski, and the weighting scheme, (uniform or distance). The used hyperparameteres were based on documented values from [130], and can be seen in Table 12. The number of neighbours was chosen based on an interactive process, where several values were tested.

Table 12- Hyperparameteres for the KNN classifier

n_neighbors	7
weights	uniform
algorithm	auto
leaf_sie	30
p	2
metric	minkowski
metric_params	None
n_jobs	None

5.4.4.3 Decision Tree (DT)

DecisionTreeClassifier was implemented using scikit-learn. This classifiers hyperparameters included the splitting criterion (gini impurity or entropy), maximum depth (max_depth), minimum samples required to split a node (min_samples_ split), and minimum samples require data leaf node (min_samples_leaf). The used hyperparameters were based on documented values [131], and can be found in Table 13.

Table 13- Hyperparameteres for the DT classifier

criterion	gini
splitter	best
max_depth	None
min_samples_split	2
min_samples_leaf	1
min_weight_fraction_leaf	0
max_features	None
random_state	None
max_leaf_nodes	None
min_impurity_decrease	0
class_weigth	None
ccp_alpha	0
montonic_cst	None

5.4.4.4 Random Forest (RF)

The RF ensemble was implemented with scikit-learn's RandomForestClassifier. RF aggregate predictions from many decision tree estimators, which tends to yield more stable probability estimates than a single tree, so there was no need for additional calibration. The hyperparameter for RF included the number of trees, maximum tree depth (max_depth), minimum samples for splits and leaves and the number of features considered when splitting each node. The used hyperparameters were based on documented values [132] and can be found in Table 14.

Table 14- Hyperparameteres for the RF classifier

n_estimators	100
criterion	gini
max_depth	None
min_samples_split	2
min_samples_leaf	1
min_weight_fraction_leaf	0
max_features	sqrt'
max_leaf_nodes	None
min_impurity_decrease	0
bootstrap	True
oob_score	False
n_jobs	None
random_state	None
verbose	0
warm_start	False
class_weight	None
ccp_alpha	0
max_sampls	None
monotonic_cst	None

5.4.4.5 Naive Bayes

The variant used in this study was the Guassian NB. The hyperparametrs of this classifier include prior probabilities of the classes (priors) and variance smoothing (var_smoothing). The used hyperparameters were based on documented values [133], and can be seen in Table 15.

Table 15- Hyperparameters of the GaussianNB classifier

Priors	**None**
Var_smoothing	**1e-09**

5.4.4.6 Logistic Regression

LR was applied using scikit-learn's LogisticRegression class. This linear model predicts the

probability of the positive class via the logistic (sigmoid) function applied to a linear combination of features. The hyperparameters used were based on documented values [134], and can be seen in Table 16.

Table 16- Hyperparameters of the LR classifier

penalty	deprecated
C	1
l1_ratio	0
dual	False
tol	0,0001
fit_intercept	True
intercept_scaling	1
class_weight	None
random_state	None
solver	lbfgs
max_iter	10000
verbose	0
warm_start	False
n_jobs	None

5.4.4.7 Extreme Gradient Boost (XGB)

This classifier was implemented with the xgboost library. The main parameter to set is the type of booster used. For this study, the logarithmic booster was used. The hyperparameters were based on documented values [135].

5.4.4.8 Long Short term memory (LSTM)

The LSTM classifier was applied with the tensorflow library. The hyperparameters of this classifier include the number of units, the number of epochs, the loss function, the batch size and the optimizer. The used hyperparameters were based on documented values [136], and can be seen in Table 17.

Table 17- Hyperparameters used for the LSTM classifier

units	128
return_sequences	True
Dropout	0,2
LSTM units	128
Dropout	0,2
Dense	1
optimizer	adam
loss	mean_square_error
epochs	100
batch_size	32
validation_split	0,1

6
RESULTS AND DISCUSSION

Table 18, Table 19, Table 20 and Table 21 present the results from the analysis of the entire dataset, comparing gait parameters between PD patients and HC, for each gait task: FrW, DTW, OBW and FaW. This initial exploration was made in order to capture the group differences across tasks and between the two groups. The values were considered statistically diferent for a value of P equal or smaller than the 0.05.

Table 18- Gait parameters, ObW

	PD mean± std	**HC mean±std**	**P**
Step length mean	57.20±13.41	63.71±8.01	0.34
Step time mean	0.63±0.15	0.55±0.63	<0.01*
Step velocity mean	96.57±32.43	118.12±19.02	0.41
Step width mean	10.47±3.76	10.85±2.93	0.40
Double support mean	0.23±0.30	0.18±0.06	<0.01*
Step length asymmetry	0.75± 4.36	0.51±3.49	0.91
Step time asymmetry	0.005 ±0.04	-0.006±0.02	<0.01*
Step velocity asymmetry	-5.06± 10.66	2.24±6.60	0.25
Step width asymmetry	-0.07 ±6.54	0.17±2.29	0.47
Double support asymmetry	-0.007± 0.04	-0.002±0.01	<0.01*

*Indicates values that have a statistically significant difference (P<0.05)

Table 19- Gait parameters, FrW

	PD mean± std	HC mean±std	P
Step length mean	56.99±9.94	65.57±7.32	0.18
Step time mean	0.54±0.08	0.54±0.053	<0.01*
Step velocity mean	109.51 ±39.94	121.70±17.85	0.46
Step width mean	10.71±3.55	11.29±2.99	0.34
Double support mean	0.18±0.15	0.18±0.06	0.03*
Step length asymmetry	1.20±4.37	0.49±2.42	0.61
Step time asymmetry	0.009±0.03	-0.003±0.02	<0.01*
Step velocity asymmetry	5.07±11.13	1.83±5.47	0.71
Step width asymmetry	3.66±5.10	1.05±2.13	0.13
Double support asymmetry	0.004±0.03	-0.002±0.02	<0.01*

*Indicates values that have a statistically significant difference (P<0.05)

Table 20- Gait parameters, DTW

	PD mean± std	HC mean±std	P
Step length mean	54.19±8.81	65.86±6.37	0.10
Step time mean	-0.24±3.50	0.97±6.37	0.19
Step velocity mean	0.55±0.05	0.55±0.06	0.42
Step width mean	-0.0009±0.03	-0.005±0.02	<0.01*
Double support mean	99.55±18.62	120.76±16.96	0.35
Step length asymmetry	-0.14±7.79	2.93±5.25	0.32
Step time asymmetry	11.93±3.13	12.69±2.61	0.29
Step velocity asymmetry	0.74±5.01	1.62±2.24	0.35
Step width asymmetry	0.16±0.03	0.16±0.03	<0.01*
Double support asymmetry	0.003±0.02	-0.003±0.01	<0.01*

*Indicates values that have a statistically significant difference (P<0.05)

Table 21- Gait parameters, FaW

	PD mean± std	HC mean±std	P
Step length mean	66.11±12.66	75.88±9.90	0.35
Step time mean	-2.58±4.23	0.99±2.60	0.04*
Step velocity mean	0.60±0.51	0.47±0.05	<0.01*
Step width mean	-0.01±0.03	-0.006±0.02	<0.01*
Double support mean	142.37±34.77	162.09±24.60	0.45
Step length asymmetry	-0.29±10.72	4.72±8.76	0.40
Step time asymmetry	10.59±4.03	12.22±2.61	0.20
Step velocity asymmetry	3.04±9.26	2.59±2.23	0.94
Step width asymmetry	0.44±4.17	0.11±0.03	0.80
Double support asymmetry	-0.004±0.03	-0.008±0.01	<0.01*

*Indicates values that have a statistically significant difference (P<0.05)

6.1 SPATIOTEMPORAL PARAMETERS

Across all sections, PD patients present an average lower step velocity and a shorter step length compared to controls, which is consistent with the findings reported in literature. However, the differences in these values are not statistically significate. O the other hand, the step time and the double support present statistically significant differences on every walking task, with a bigger accentuation in dual tasking and fast walking.

The asymmetry of the step length, step velocity and step width didn't present statistically significant differences between groups. However, the asymmetry of the step time and double support was statistically different in every walking task.

6.2 Dataset Processing

Patterns of missingness, and normalisation consistency were observed in dataset, as mentioned before. The dataset shows a considerable amount of missing values across the different gait tasks, particularly in OBW and FaW, where several features presented high percentages of missing entries. In contrast, FrW and DTW showed lower and more localised missingness. In order to be able to use all the available data, it becomes necessary to apply techniques that fill in the missing values, such as CTGAN.

Figure 24 presents the number of available data without missing values for each walking task, before and after the CTGAN was applied.

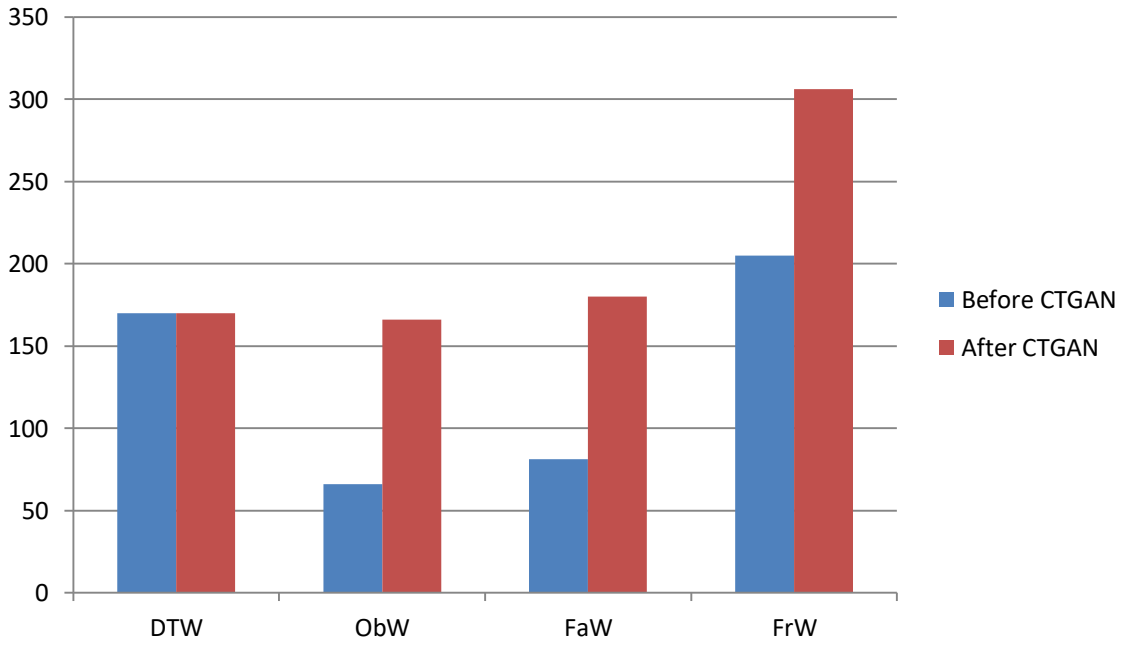


Figure 24- Complete available data before and after the application of CTGAN

The different scales used in the rating of the different features made it a requirement the use of normalisation processes. The one used in this study was the minmax scale. The effects of normalization may be seen in Figure 25,

Figure 26,

Figure 27 and Figure 28.

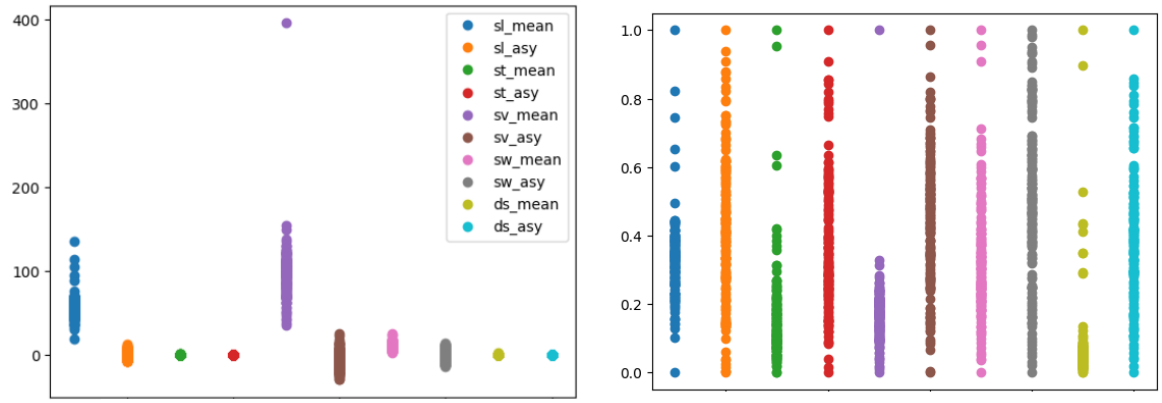


Figure 25- Distribution of the spatiotemporal parameters for ObW, before (on the left) and after (on the right) of the application of the minmax scale

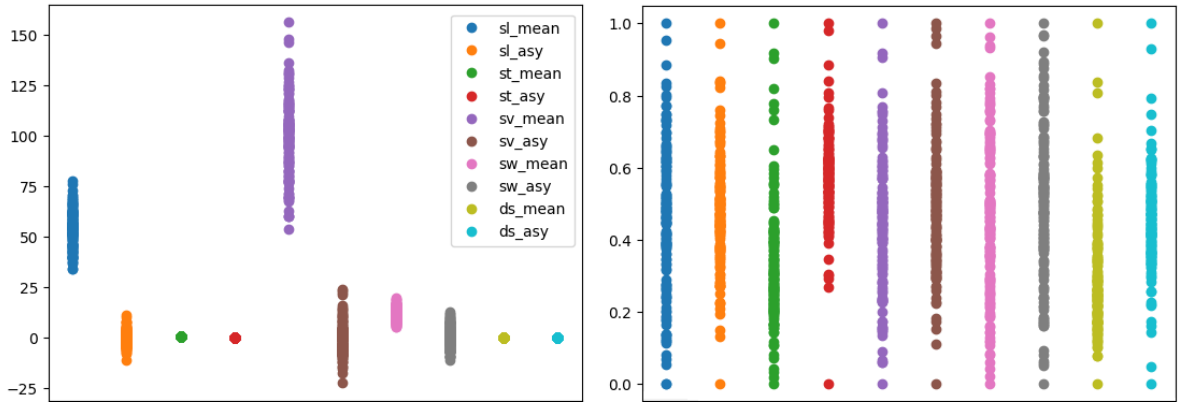


Figure 26- Distribution of the spatiotemporal parameters for DTW, before (on the left) and after (on the right) of the application of the minmax scale

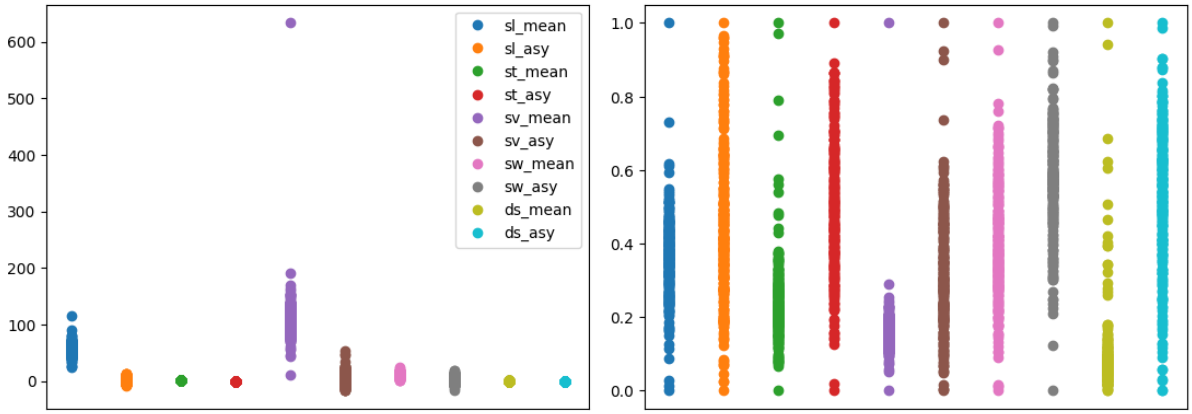


Figure 27- Distribution of the spatiotemporal parameters for FrW, before (on the left) and after (on the right) of the application of the minmax scale

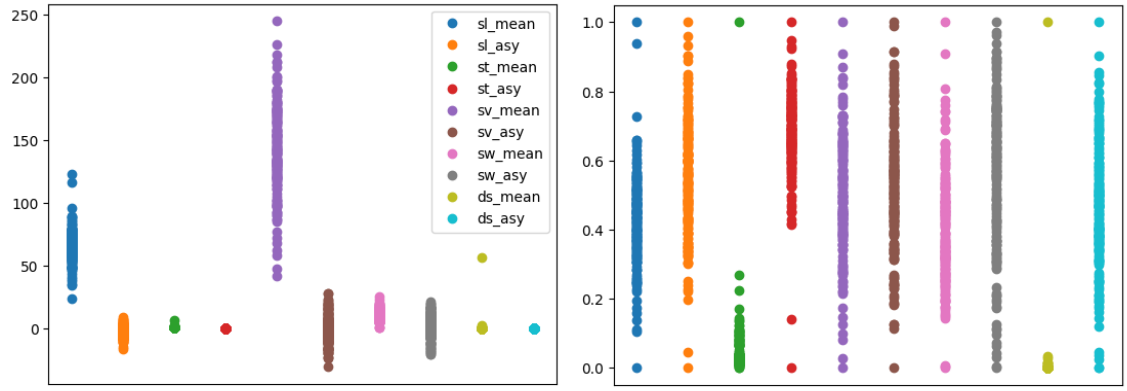


Figure 28- Distribution of the spatiotemporal parameters for FaW, before (on the left) and after (on the right) of the application of the minmax scale

6.3 Models Results

6.3.1 All features

For the purpose of this study, several ML and DL algorithms were tested in the ability to distinguish PD patients from a HC group. The results obtained by the tested algorithms after normalisation and applying the SMOTE technique are shown for each task in Figure 29.

The best overall results were achieved by the XGB algorithm, with the Fast Walking dataset. This algorithm achieved an accuracy of 98.61%, a F1-score of 98.59%, a recall of 97.22% and a precision of 100%.

Considering the average of the results regarding all the walking tasks, the XGB algorithm has the best performance overall, with relatively high values on accuracy, F1-score, recall and precision. The overall worst performance was made by the LR algorithm. A comparison between the average results of every algorithm, regarding all the walking tasks is shown in .

Regarding the walking tasks performed by the participants, the best results were generally obtained with data from the DTW, while the worst results were obtained with the OBW. An analysis of the overall performance of each sub dataset is shown in Figure 30.

It was also noticeable that precision values were generally higher than the recall values, which indicated that the number of false positives was generally low, compared to the false negatives.

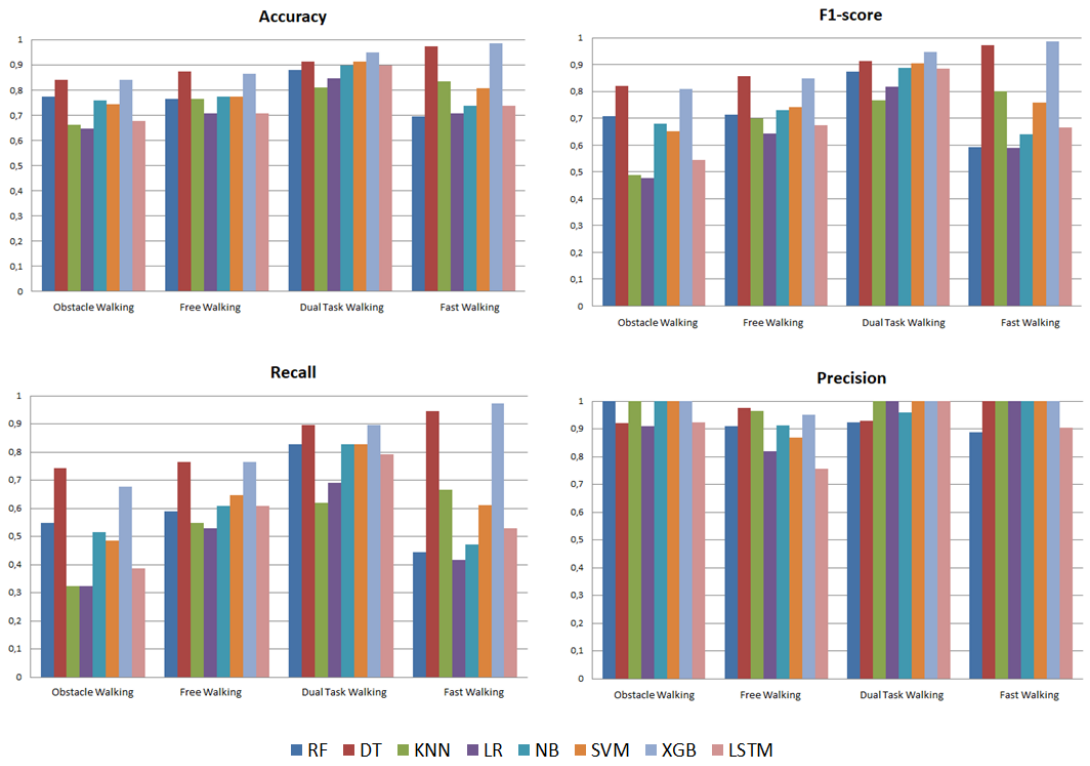


Figure 29- Results of the ML and DL models. All the features.

	Acc	F1	Rec	Pres
RF	0,778164	0,721985	0,602163	0,930264
DT	0,899319	0,89057	0,836909	0,955893
KNN	0,767419	0,688441	0,539739	0,991379
LR	0,726051	0,630902	0,489579	0,931818
NB	0,791309	0,735165	0,605945	0,967941
SVM	0,808948	0,764507	0,642407	0,967105
XGB	0,90896	0,896722	0,827725	0,987805
LSTM	0,753991	0,692662	0,578955	0,895984

	Acc	F1	Rec	Pres
ObW	0,741935	0,647491	0,5	0,969021
FrW	0,774628	0,722319	0,60476	0,915284
DTW	0,887931	0,873989	0,797414	0,976456
FaW	0,809028	0,750621	0,631944	0,974206

Figure 30- Average performance of the models and the sub datasets without feature selection

6.3.2 Feature Selection

Regarding the feature selection, each walking tasks went through three different selection processes, with three different algorithms: WOA, PSO and SMA. Overall, a total of 12 sub datasets was tested. The results obtained for the algorithm performance are seen in figures below.

6.3.2.1 Slime Mould Algorithm

The features selected with the SMA algorithm are summoned in Table 9. The best performance was achieved by the XGB algorithm with the FaW dataset. An accuracy of 95.83% was obtained, as well as an F1-score of 95.77%, a recall of 94.4% and a precision of 97.14%. Although this result is very promising, the model performance appeared to decline with the application of the feature selection, which may imply that this isn't the ideal method considering the data used in this study.

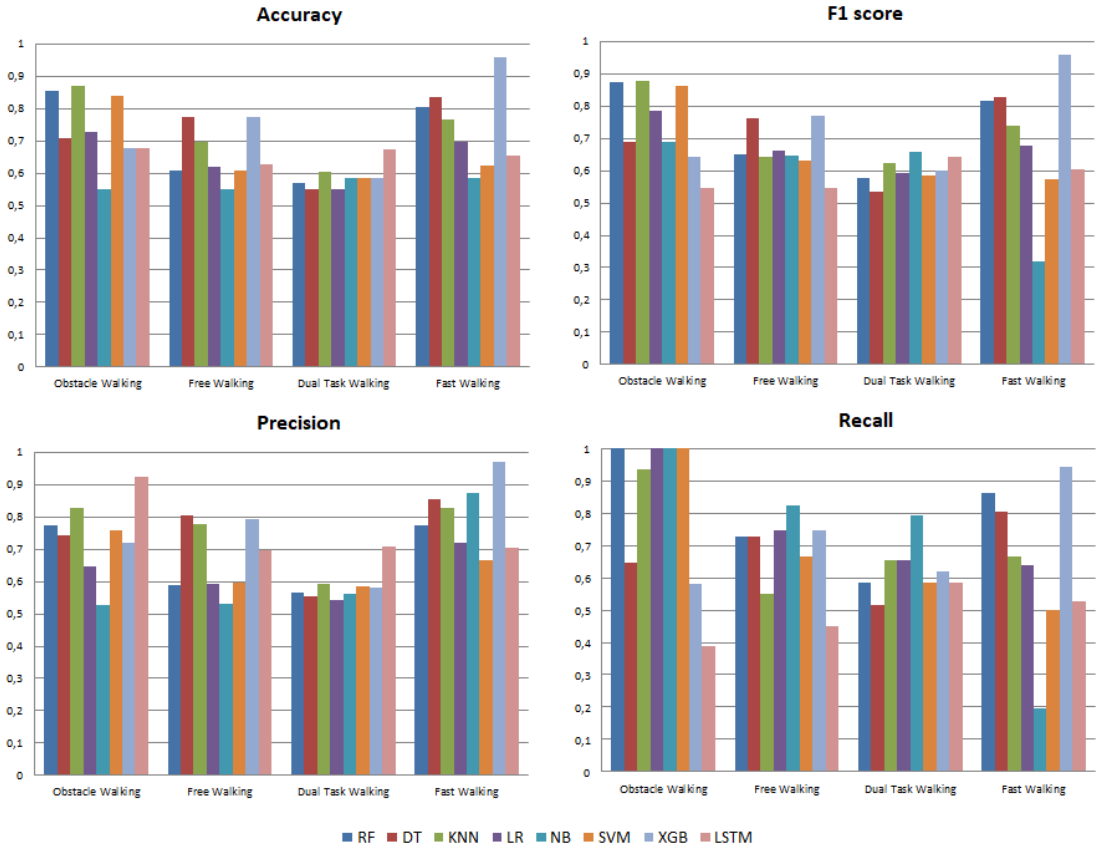


Figure 31- Overall results from applied algorithms after SMA feature selection is applied

	Acc	F1-score	Recall	Precision
RF	0,709301	0,728606	0,793202	0,675992
DT	0,717311	0,704207	0,673362	0,738396
KNN	0,733596	0,72097	0,701586	0,756921
LR	0,647406	0,678975	0,75979	0,625298
NB	0,566737	0,577592	0,702769	0,623261
SVM	0,66444	0,662094	0,688218	0,651366
XGB	0,749117	0,74207	0,722719	0,765935
LSTM	0,657515	0,584439	0,488015	0,758021

	ObW	FrW	DTW	FaW
Acc	0,7379	0,65686	0,58836	0,73958
F1-score	0,7456	0,66345	0,60169	0,68873
Recall	0,81855	0,67892	0,625	0,64236
Precision	0,73934	0,67249	0,58687	0,79888

Figure 32- Overall performance of the models and the sub datasets after SMA feature selection

6.3.2.2 Particle Swarm optimization

The features selected with the PSO method are shown in Table 8. The general performance of the algorithms declined with the application of PSO feature selection, not only in comparison with the models using all features, but also in comparison with the SMA feature selection, implying that the PSO method is also inadequate for the dataset used in this study. The best performances were in general obtained by the LSTM network and the XGB algorithm, with the best result being achieved by the XGB for the Fast Walking dataset. An accuracy of 95.83 % was obtained, as well as a F1-score of 95.77%, a recall of 94.44% and a precision of 97.14%.

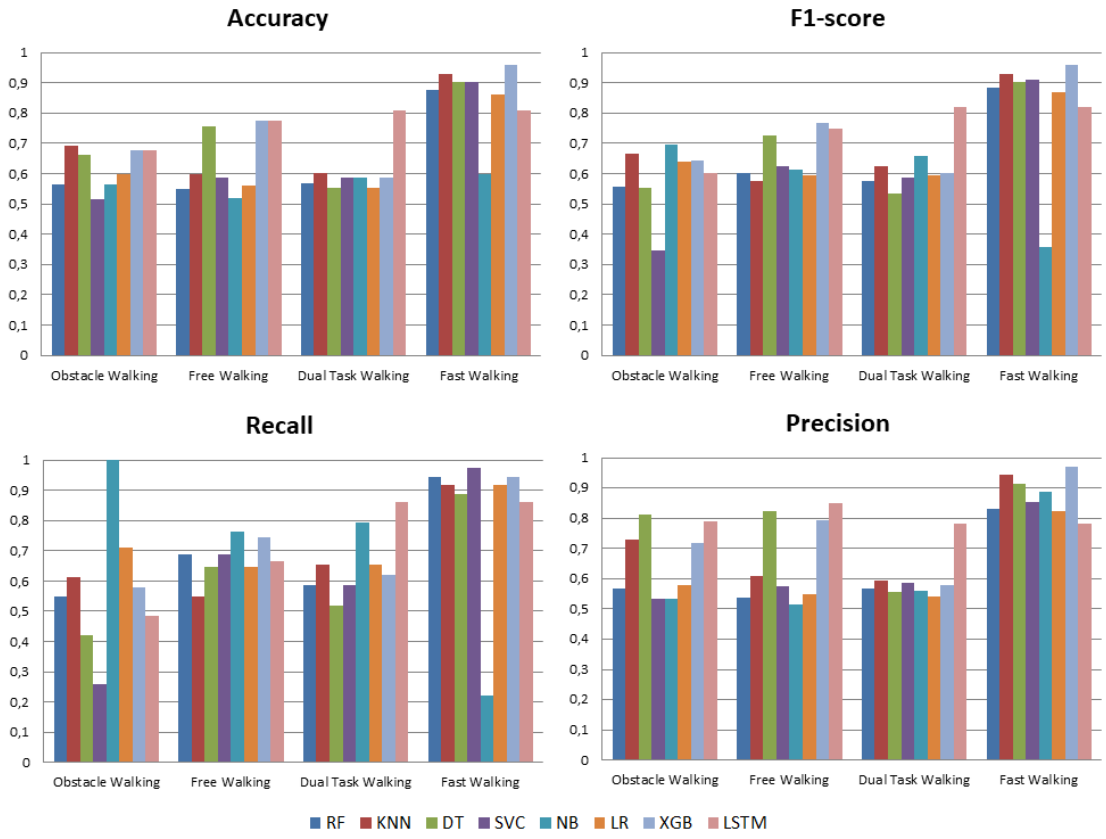


Figure 33- Results obtained by the models after PSO feature selection is applied

	ObW	FrW	DTW	FaW
RF	0,639375	0,655053	0,691328	0,625266
KNN	0,706398	0,699129	0,68344	0,719018
DT	0,717674	0,678897	0,618136	0,776835
SVC	0,648337	0,617031	0,625692	0,636742
NB	0,566888	0,580875	0,695008	0,624376
LR	0,642108	0,673612	0,732144	0,624201
XGB	0,749117	0,74207	0,722719	0,765935
LSTM	0,768155	0,746649	0,718669	0,800493

	ObW	FrW	DTW	FaW
Acc	0,618952	0,639706	0,605603	0,854765
F1-score	0,587779	0,656842	0,623964	0,828074
Recall	0,576613	0,67402	0,659483	0,833453
Precision	0,658272	0,656344	0,595988	0,87583

Figure 34- performance of the algorithms and the datasets after PSO was applied.

6.3.2.3 Whale Optimization Algorithm

Regarding the WOA feature selection, the performance of the models achieved its lowest performance when this method was used. The used features are shown in Table 10. Unlike what was verified with the other features, the XGB didn't present such a good performance when these features were used. The best overall performance was achieved by the LSTM network, with the best result being achieved for the Fast Walking dataset. The best

performance obtained an accuracy of 86%, an F1-score of 86%, a recall of 83% and a precision of 88%.

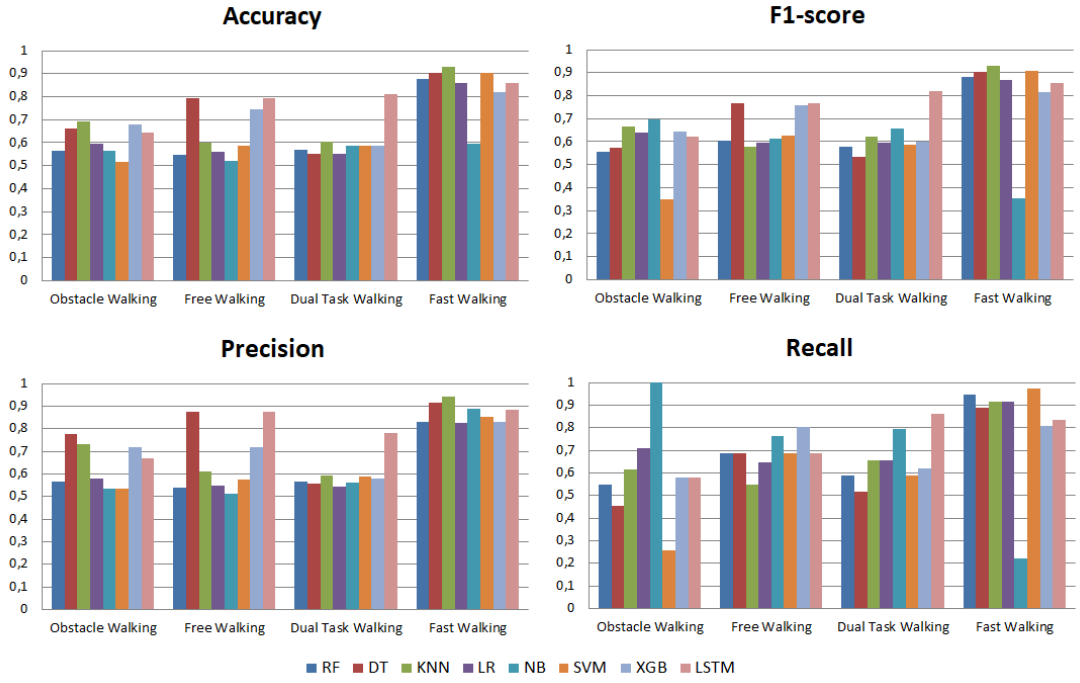


Figure 35- Results obtained by the models after WOA feature selection is applied.

	Acc	F1-socre	Recall	Precision
RF	0,63938	0,65505	0,69133	0,62527
DT	0,72748	0,69445	0,636	0,78065
KNN	0,7064	0,69913	0,68344	0,71902
LR	0,64211	0,67361	0,73214	0,6242
NB	0,56689	0,58088	0,69501	0,62438
SVM	0,64834	0,61703	0,62569	0,63674
XGB	0,70704	0,70475	0,7027	0,71213
LSTM	0,77768	0,76668	0,74058	0,80132

	ObW	FrW	DTW	FaW
Acc	0,61492	0,59264	0,59274	0,63858
F1-score	0,62212	0,59768	0,59908	0,64885
Recall	0,67051	0,80176	0,96313	1,10917
Precision	0,66667	0,82428	1,02151	1,17224

Figure 36- Performance of the algorithms and the datasets after WOA was applied.

In conclusion, in the model presented with all the features, the best performances were achieved with the dual Task walking dataset, while after the application of feature selection, the best results were achieved by the fast Walking Dataset, which leads to believe that the feature selection enhanced features that have a higher statistic difference between the two groups of participants.

The SMA revealed to be the feature selection algorithm with the best results, although the overall performance of the algorithms after the feature selection decreased when compared to the algorithms that used all the features, which implies that the feature selection methods used in this study weren't ideals.

The XGB algorithm and the LSTM network demonstrated to have the best results in all the cases, which enlightens the potential of these algorithms to improve PD diagnose and be assisting to doctors.

The tested models shown promising results, and contain the potential to become a useful tool to humiliate health care professionals in the diagnose of PD and in the improvement of patient treatment.

7
CONCLUSION AND FUTURE WORK

This thesis investigated the potential of gait as a robust digital biomarker for Parkinson's disease, combining a comprehensive systematic review of the literature with the development and evaluation of a broad set of machine learning and deep learning models. The review revealed a rapidly evolving research landscape, marked by increasing interest in automated PD detection, yet still characterised by methodological heterogeneity, limited dataset sizes, and inconsistent evaluation practices. By mapping model families, dataset characteristics, and validation strategies, this work clarified the trade-offs between traditional ML approaches—more interpretable and computationally efficient—and DL architectures, which excel at learning complex spatiotemporal patterns but require larger datasets and careful regularisation.

Building on these insights, the experimental framework implemented in this thesis provided a unified and reproducible environment for benchmarking PD detection models. Classical ML classifiers, an LSTM neural network, and several feature engeneering methods were rigorously compared under controlled conditions. The results demonstrated that ML and DL methods offer a promising path toward more generalisable and scalable PD detection systems, particulary the XGB algorithm, tha consistently exhibited the best performace towards almost every one of the studied scenarios. The framework developed here thus contributes not only empirical findings but also a methodological reference for future studies.

The feature engeneering methods tested in this thesis didn't provide an improvement in the results. Since al the tested methods were meta heucaristsic, they didn't present the optimal solution, but rather a "good" solution that fitted the stopping criteria. A bigger amount of attempts for each algorithm increases the possibility to find the optimal solution. Since only three attemps were performed for each algorithm when this work was conducted, it's possible that the amount of attemps wasn't sufficient to find the optimal solution.

Overall, this thesis reinforces the value of gait analysis as a non-invasive, accessible, and clinically meaningful digital biomarker. At the same time, it highlights the need for methodological standardisation, larger and more diverse datasets, and stronger clinical validation to ensure that algorithmic advances translate into real-world impact.

Future work should include the exploration of additional feature-engineering techniques better suited to the characteristics of the dataset, or the application of the algortihms used in this work with a higher amount of attempts, in order to increase the possibility to find the optimal solution, as well as the investigation of multimodal approaches that combine complementary biomarkers such as voice, handwriting, and tremor signals. Another promising direction is the development of ensemble models that integrate multiple traditional ML classifiers to enhance robustness and generalisation. Finally, future research should extend the use of machine learning beyond binary diagnosis, applying these methods to disease staging and progression assessment, which would provide greater clinical relevance and support personalised patient monitoring.

REFERENCES

[1] S. Asmi, A. Krishnan, S. M. Alexander, J. Mohamed Ameer, T. Nidhish, S. C. Sreetama, T. Keerthi, R. A. Shenoi, S. S. Chakravarthy and G. Chandra, "An update on the monogenic causes of Parkinson's disease: Impact on patient stratification and personalised medicine," *Ageing Research Reviews,* vol. 118, p. 103070, 2026-06-01.

[2] C. F. Ana Margarida, "Parkinson's Disease Detection Based On Visual Speech," Master Thesis, Técnico de Lisboa, 2023.

[3] M. T. Hayes, "Parkinson's Disease and Parkinsonism," *The American Journal of Medicine,* vol. 132, pp. 802-807, 2019.

[4] J. Jankovic, "Parkinson's disease: clinical features and diagnosis," *J Neurol Neurosurg Psychiatry,* vol. 79, pp. 368-376, 2008.

[5] D. P. O'Brien and G. C. Johnson, "Dysautonomia and autonomic neuropathies," *Veterinary Clinics of North America: Small Animal Practice,* vol. 32, pp. 251-265, 2002.

[6] G. A. Cook, J. T. Kissel and M. M. Dimachkie, "Autonomic Neuropathies," *Neurologic Clinics,* vol. 43, pp. 851-872, 2025.

[7] N. C. B. S. Silva, G. M. Balbim, R. S. Falck and T. Liu-Ambrose, "Physical activity interventions in cognitive aging," *Encyclopedia of the Human Brain,* pp. 82-94, 2025.

[8] S. P. Chand and H. Arif, "Depression," *StatPearls,* 2023.

[9] American Psychological Association, "APA Dictionary of Psychology," 4 19 2018. [Online]. Available: https://dictionary.apa.org/anxiety. [Accessed 23 04 2026].

[10] M. Menza, R. D. Dobkin, H. Marin and K. Bienfait, "Sleep Disturbances in Parkinson's Disease," *Movement Disorders,* vol. 25, pp. S117-S122, 2010.

[11] L. B. Zahodne and H. H. Fernandez, "Parkinson's Psychosis," *Current Treatment Options in Neurology,* vol. 12, pp. 200-11, 2010.

[12] K. Radad, R. Moldzio, C. Krewenka, B. Kranner and W.-D. Rausch, "Pathophysiology of non-motor signs in Parkinson's disease: some recent updating with brief presentation," *Exploration of Neuroprotective Therapy,* vol. 3, pp. 24-46, 2023.

[13] M. Tinelli, P. Kanavos and F. Grimaccia, "THE VALUE OF EARLY DIAGNOSIS AND TREATMENT IN PARKINSON'S DISEASE," in *The Role Of EU Public Health & Social Policies In Improving Quality Of Life*, European Parliament, Brussels, 2017.

[14] S. Yandrapalli and Y. Puckett, "SPECT Imaging," *StatPearls [Internet],* 2022.

[15] U. Walter, "Transcranial sonography of the cerebral parenchyma: Update on clinically relevant applications," *Perspectives in Medicine,* vol. 1, pp. 334-343, 2012.

[16] G. Gusinu, C. Frau, G. A. Trunfio, P. Solla and L. A. Sechi, "Segmentation of Substantia Nigra in Brain Parenchyma Sonographic Images Using Deep Learning," *Journal of Imaging,* vol. 10, 2023.

[17] D. Smajlovic and O. C. Ibrahimagic, "Transcranial Brain Sonography in Parkinson's Disease and Other Parkinsonian Disorders: a Hospital Study from Tuzla, Bosnia and Herzegovina," *Medical Archives,* vol. 71, pp. 261-264, 2017.

[18] T. Yousaf, G. Dervenoulas and M. Politis, "Chapter Two - Advances in MRI Methodology," in *International Review of Neurobiology,* 2018, pp. 31-76.

[19] J. S. Perlmutter, "Assessment of Parkinson Disease Manifestations," *Current protocols in neuroscience,* 2009.

[20] J. Jankovic and L. G. Aguilar, "Current approaches to the treatment of Parkinson's disease," *Neuropsychiatric Disease and Treatment,* vol. 4, pp. 743-757, 2008.

[21] N. Malek, "Deep Brain Stimulation in Parkinson's Disease," *Neurology India,* vol. 4, pp. 968-978, 2019.

[22] NHS, "Parkinson's disease - Treatment - NHS," [Online]. Available: https://www.nhs.uk/conditions/parkinsons-disease/treatment/. [Accessed 15 05 2026].

[23] D. L. Murman, "Early Treatment of Parkinson's Disease: Opportunities for Managed Care," *Best Practices for Treating Parkinsona's Disease: A Focus on Symptoms and Considerations for Manage,* vol. 18, 2012.

[24] C. Kruse, A. Lipinski, M. Verheyen, M. Balzer-Geldsetzer, M. Wittenberg, S. Lorenzl, C. Richinger, C. Schmotz, L. Tönges, D. Woitalla, S. Klebe, B. R. Bloem, A. Hommel, W. G. Meissner, B. Laurens, T. Boraud, A. Foubert-Samier, S. Vergnet, F. Tison, N. Costa, P. Odin, K. Rosqvist, J. M. Norlin, F. Hjalte, A. Schrag and R. Dodel, "Care of Late-Stage Parkinsonism: Resource Utilization of the Disease in Five European Countries," *Movement Disorders,* vol. 39, pp. 571-584, 2024.

[25] D. Sethi, S. Bharti and C. Prakash, "A comprehensive survey on gait analysis: History, parameters, approaches, pose estimation, and future work," *Artificial Intelligence in Medicine,* vol. 129, 2022.

[26] A. Mirelman, S. Shema, I. Maidan and J. M. Hausdorff, "Chapter 7 - Gait," in *Handbook of Clinical Neurology,* Elsevier, 2018, pp. 119-134.

[27] K. Chekka, J. D. Moore and H. T. Benzon, "Chapter 4 - Physical examination of the patient with pain," in *Essentials of Pain Medicine,* 2011, pp. 19-27.

[28] S. M. Kim, D. H. Kim, Y. Yang, S. W. Ha and J. H. Han, "Gait Patterns in Parkinson's Disease with or without Cognitive Impairment," *Dementia and Neurocognitive Disorders,* vol. 17, pp. 57-65, 2018.

[29] J. G. Nutt, B. R. Bloem, N. Giladi, M. Hallett, F. B. Horak and A. Nieuwboer, "Freezing of gait: moving forward on a mysterious clinical phenomenon," *Lancet Neurology,* vol. 10, pp. 734-744, 2020.

[30] I. H. Sarker, "Machine Learning: Algorithms, Real-World Applications and Research Directions," *Sn Computer Science,* vol. 2, p. 160, 2021.

[31] H. Hamjad, "Machine Learning Introduction: KNN Model," 7 10 2024. [Online]. Available: https://www.mssqltips.com/sqlservertip/8096/machine-learning-introduction-knn-model/. [Accessed 13 6 2026].

[32] S. B. Jabeur, C. Gharib, S. Mefteh-Wali and W. B. Arfi, "CatBoost model and artificial intelligence techniques for corporate failure prediction," *Technological Forecasting and Social Change,* vol. 166, 2021.

[33] R. Y. Choi, A. S. Coyner, J. Kalpathy-Cramer, M. F. Chiang and J. P. Campbell, "Introduction to Machine Learning, Neural Networks, and Deep Learning," *Translational vision science & technology,* vol. 9, 2020.

[34] I. Malashin, V. Tynchenko, A. Gantimurov, V. Nelyub and A. Borodulin, "Applications of Long Short-Term Memory (LSTM) Networks in Polymeric Sciences: A Review," *Polymers,* vol. 16, p. 2607, 2024.

[35] S. Das, A. Tyagi, S. D. K, B. C and J. P, "Early Detection of Parkinson's Disease Based on Voice Disorders Using Deep Learning," in *International Conference on Biomedical Engineering and Sustainable Healthcare*, Manipal, India, 2025.

[36] S. M. M. U. Rahman, S. Mondol, A. M. Khan and S. naaz, "A Detailed Study on Efficiency of ML Based Algorithms in Predicting Parkinson's Disease Using Audio," in *2025 3rd International Conference on Disruptive Technologies (ICDT)*, 2025.

[37] S. Soltana, T. Tabassum and N. Mamun, "Speech-based Parkinson's Disease Detection with Hybrid Machine Learning Approach," in *2025 International Conference on Electrical, Computer and Communication Engineering (ECCE)*, Chittagong, Bangladesh, 2025.

[38] A. Alrosan, M. Abdel-Aty, M. Hafez, S. Alkhazaleh, M. A.Deif and R. ELGohary, "Parkinson's Disease Detection Based on Vocal Biomarkers and Machine Learning Approach," in *2024 International Telecommunications Conference (ITC-Egypt)*, Cairo, Egypt, 2024.

[39] S. P. J, J. S, L. A, N. M. B and K. S, "Exploring Voice Feature Variations in Parkinson's Disease Prediction with Machine Learning," in *2025 Third International Conference on Networks, Multimedia and Information Technology (NMITCON)*, BENGALURU, India, 2025.

[40] J. Basavaiah, A. A. Anthony, L. H. R, P. N, L. S and M. S. B, "Voice Biomarkers-Based Prediction of Parkinson's Disease Using Multiple Machine Learning Techniques," in *2025 International Conference on Communication, Computer, and Information Technology (IC3IT),* Mandya, India, 2025.

[41] I. Tougui, M. Zakroum, O. Karrakchou and M. Ghogho, "PD-VOST: Parkinson's Disease Voice Spectrogram Transformer," in *ICASSP 2025 - 2025 IEEE International Conference on Acoustics, Speech and Signal Processing (ICASSP)*, Hyderabad, India, 2025.

[42] V. Tailwal, S. Ghosh, A. Ghosh, B. Dubey and N. D. Jana, "Speech-Based Efficient Parkinson's Disease Detection Using Hybrid Deep Learning Framework," in *2025 IEEE 9th International Conference on Information and Communication Technology (CICT)*, Chennai, India, 2025.

[43] D. Quamar, V. D. A. Kumar, M. Rizwan, O. Bagdasar and M. Kadar, "Voice-Based Early Diagnosis of Parkinson's Disease Using Spectrogram Features and AI Models," *Artificial Intelligence in Neurodegenerative Disorders: Advances in Diagnosis, Prognosis and Treatment,* vol. 12, p. 1052, 2025.

[44] M. Dudek, D. Hemmerling, M. Kaczmarska, J. Stepien, M. Daniol, M. Wodzinski and M. Wojcik-Pedziwiatr, "Analysis of Voice, Speech, and Language Biomarkers of Parkinson's Disease Collected in a Mixed Reality Setting," *Advanced Wearable Sensors and Other Sensing Technologies for Diagnosis and Treatment of Parkinson's Disease and Movement Disorders,* vol. 25, p. 2405, 2025.

[45] S. S. Nayak, A. D. Darji, P. K. Shah and J. R. Orozco-Arroyave, "Automatic detection of Parkinson's disease from speech signals using the Fourier–Bessel domain adaptive wavelet transform," *Applied Acoustics,* vol. 245, p. 111217, 2026.

[46] R. Kumari and P. Ramachandran, "Novel multistage deep convolution neural network-based Parkinson's disease detection and severity grading of running speech using LSF spectrums for detection and STFT spectrums for grading," *Results in Engineering*, vol. 27, p. 106642, 2025.

[47] P. Durga, A. B. M. Ali, D. Godavarthi, S. N. Mohanty, S. Formanova and M. I. Khan, "An ensemble model for detection of Parkinson's disease by comparing numerous machine learning models and XGBoost based on vocal features," *Clinical eHealth*, vol. 8, pp. 273-287, 2025.

[48] A. N. Tekindor and E. A. Aydın, "Speech signals-based Parkinson's disease diagnosis using hybrid autoencoder-LSTM models," *Computers in Biology and Medicine*, vol. 193, p. 110334, 2025.

[49] L. Aversano, M. Iammarino, A. Madau, D. Montano and C. Verdone, "Explainable Approach For Early Diagnosis of Parkinson's Using Audio Tracks," *Procedia Computer Science*, vol. 270, pp. 3728-3737, 2025.

[50] J. A. Qadir, "Enhancing Parkinson's Disease Detection by Combining SMOTE and Feature Selection for Improved Machine Learning Classification Using Voice Recordings," *Journal of Voice*, 2025.

[51] M. H. Mohammed, M. N. Kadhim, D. Al-Shammary and A. Ibaida, "Novel Voice Signal Segmentation Based on Clark Distance to Improve Intelligent Parkinson Disease Detection," *Journal of Voice*, 2025.

[52] P. Pathak, S. Akashe and G. M. Upadhyay, "Early detection of Parkinson's disease through supervised machine learning techniques on voice data," *Informatics in Medicine Unlocked*, vol. 59, p. 101705, 2025.

[53] D. Amilo, K. Sadri, E. Hincal and M. Hafez, "A hybrid computational framework for Parkinson's disease prediction using fractional-order modeling and machine learning via vocal biomarkers," *Ain Shams Engineering Journal*, vol. 17, p. 103889, 2026.

[54] M. Chakole, S. Dorle, R. Agrawal, P. Dasarwar, U. Yadav and R. Sharma, "Vocal features based Parkinson's detection: An ensemble learning approach," *MethodsX*, vol. 15, p. 103662, 2025.

[55] R. Singh, D. Goyal, S. Arora, J. Malviya and D. Garg, "Evaluating the Severity of Parkinson's Disease Using Machine Learning Classifiers," in *2025 International Conference on Cognitive Computing in Engineering, Communications, Sciences and Biomedical Health Informatics (IC3ECSBHI)*, Greater Noida, India, 2025.

[56] M. Chahar and D. Vetrithangam, "Efficient Detection of Parkinson's Disease Using Deep Learning," in *2025 IEEE 4th International Conference for Advancement in Technology (ICONAT)*, Goa, India, 2025.

[57] T. Dalal, S. Mishra, J. Giri and V. Prakash, "Parkinson Detection Using Machine Learning (ML) Algorithms," in *2025 3rd International Conference on Communication, Security, and Artificial Intelligence (ICCSAI)*, Greater Noida, India, 2025.

[58] M. Kumar, V. A. Jayan, Y. Singla and A. Monga, "Enhanced Machine Learning Framework for Robust Early Detection of Parkinson's Disease," in *2025 IEEE International Conference on Intelligent Signal Processing and Effective Communication Technologies (INSPECT)*, Gwalior, India, 2025.

[59] S. Nimmala, C. Srilakshmi, N. S. Gupta, P. Narsimhulu, S. Kiran and M. Arivukarasi, "A Fuzzy-based Neurodiagnostic System for Early Detection of Parkinson's Disease using Wearable Sensor Data," in *2025 5th International Conference on Soft Computing for Security Applications (ICSCSA)*, Salem, India, 2025.

[60] P. Valarmathi, Y. Suganya, K. R. Saranya and S. S. Priya, "Enhancing parkinson disease detection through feature based deep learning with autoencoders and neural networks," *Scientific Reports,* vol. 15, p. 8624, 2025.

[61] M. Elkharadly, K. Amin, O. Abo-Seida and M. Ibrahim, "Bayesian optimization enhanced FKNN model for Parkinson's diagnosis," *Biomedical Signal Processing and Control,* vol. 100, p. 107142, 2025.

[62] A. Bashir, Y. Singh, S. Zadoo and K. H. Mir, "Parkinson's Disease Detection: A Machine Learning Based Model," *Procedia Computer Science,* vol. 259, pp. 1783-1792, 2025.

[63] R. Valarmathi, V. Sudha, G. Bagyalakshmi and V. Gomathi, "Machine Learning Models for Detection of Parkinson's Disease," in *2025 International Conference on Intelligent Computing, Information and Control Systems (ICOIICS)*, Lalitpur, Nepal, 2025.

[64] A. A. Athamneh, M. E. Farfoura and D. Rosiyadi, "A CatBoost Predictive Model for Parkinson's Disease Early Detection," in *2025 1st International Conference on Computational Intelligence Approaches and Applications (ICCIAA)*, Amman, Jordan, 2025.

[65] S. Surya, A. Aarthi and B. Bhavya, "Predictive Modeling for Parkinson's disease Diagnosis: A Machine Learning Approach," in *2025 International Conference on Data Science, Agents & Artificial Intelligence (ICDSAAI)*, Chennai, India, 2025.

[66] M. Pradhan, "PredParkinson-MLP: Parkinson Disease Prediction using Multi Layer Perceptron Neural Network," in *2025 International Conference on Machine Learning and Autonomous Systems (ICMLAS)*, Prawet, Thailand, 2025.

[67] P. D. Durga, K. C. Akshita, T. Raghu, K. Sailaja and R. Hariharan, "PARK-LDNet: A Hybrid LSTM-DBN Framework for Parkinson's Disease Prediction," in *2025 IEEE International Conference on Contemporary Computing and Communications (InC4)*, Bangalore, India, 2025.

[68] A. Maheshwari, I. Banerjee and R. Jayaraman, "Parkison Disease Prediction using Machine Learning In Healthcare," in *2025 6th International Conference on Intelligent Communication Technologies and Virtual Mobile Networks (ICICV)*, Tirunelveli, India, 2025.

[69] B. Motamedi and B. Villányi, "A novel hybrid machine learning approach for early prediction of Parkinson's disease severity using optimized feature selection and ensemble learning," *Intelligence-Based Medicine,* vol. 12, p. 100276, 2025.

[70] H. K. Kannan, M. R. Pooja and V. Ravi, "Predictive Analysis of Parkinson's Disease Using Machine Learning," *The Open Bioinformatics Journal,* vol. 18, 2025.

[71] A. K. D, P. C, K. D. S. L. Kumar and Meeradevi, "Parkinson's Disease Detection Using Machine Learning Models," in *2025 6th International Conference on Mobile Computing and Sustainable Informatics (ICMCSI)*, Goathgaun, Nepal, 2025.

[72] P. Shanmugavadivu, G. J. Kirubakaran, A. Nithya and B. Ravichandran, "Optimized Parkinson's Disease Classification on Hand Drawing Images using Transfer

Learning Models: An Exploratory Analysis," in *2025 World Skills Conference on Universal Data Analytics and Sciences (WorldSUAS)*, Indore, India, 2025.

[73] R. Nawal, N. Habib and S. Barua, "A Deep Learning Based Non-Invasive Framework for Neurodegenerative Parkinson's Disease Diagnosis from Template-Less Handwritten Shapes," in *2025 4th International Conference on Robotics, Electrical and Signal Processing Techniques (ICREST)*, Dhaka, Bangladesh, 2025.

[74] M. I. Mamun, S. Hossain and M. A. R. Ahad, "Explainable AI in Healthcare: Interpretable Detection of Parkinson's Disease from Mobile-Collected Handwriting Patterns," in *2025 IEEE 4th International Conference on Computing and Machine Intelligence (ICMI)*, MI, USA, 2025.

[75] D. Aridhi, I. H. Trimech and N. E. B. Amara, "Hybrid Approach for Parkinson's Disease Detection: Integrating Handcrafted and Deep Features from Handwriting Analysis Using a Voting Classifier," in *2025 11th International Conference on Control, Decision and Information Technologies (CoDIT)*, Split, Croatia, 2025.

[76] B. R. Punya, B. R. Kumani, I. S. Rajesh, M. A. Bharathi, C. Maithri and M. S. Krishnamurthy, "Hybrid Deep Fusion of CNN and Transformer Models for Early Parkinson's Screening from Hand-Drawn Spirals and Waves," in *2025 Third International Conference on Networks, Multimedia and Information Technology (NMITCON)*, BENGALURU, India, 2025.

[77] R. A. MTech, A. V. MSc, G. R. MTech, J. T. BTech, B. A. G. MDS, D. R. DM, V. Y. V. DM, N. K. DM, V. H. DM, P. J. BE and A. S. DM, "Deep Learning–Based Artificial Intelligence Algorithm to Classify Tremors from Hand-Drawn Spirals," *Movement Disorders: Official Journal of the Movement Disorder Society*, vol. 40, pp. 1172-1181, 2025.

[78] K. A. Shastry, "Deep Learning-Based Diagnostic Model for Parkinson's Disease Using Handwritten Spiral and Wave Images," *Current Medical Science,* vol. 45, pp. 206-230, 2025.

[79] M. Al-Jabbar, M. Alshahrani, E. M. Senan, I. Abunadi, S. A. Almalki and E. A. Alshari, "Hybrid Techniques of Multi-CNN and Ensemble Learning to Analyze Handwritten Spiral and Wave Drawing for Diagnosing Parkinson's Disease," *CMES - Computer Modeling in Engineering and Sciences,* vol. 143, pp. 2429-2457, 2025.

[80] K. Pareek, G. Jain, S. Jain and V. Bhargav, "Human Drawing-Driven Automated Evaluation for Parkinson's Disease Detection," in *2025 IEEE International Students' Conference on Electrical, Electronics and Computer Science (SCEECS)*, Bhopal, India, 2025.

[81] E. Y. Özdemir and F. Özyurt, "Elasticnet-Based Vision Transformers for early detection of Parkinson's disease," *Biomedical Signal Processing and Control,* vol. 101, p. 107198, 2025.

[82] P. M. Shanthappa, M. Bayari, G. B. Abhilash, K. V. Gokul and P. J. Ashish, "Parkinson's disease detection using inceptionV3: A Deep Shanthappalearning approach," *MethodsX*, vol. 14, p. 103333, 2025.

[83] N. Kapileswar and J. Simon, "IoT-Enabled Diagnostic Model Using Deep Learning for Early Detection of Parkinson's Disease from Gait and Brain Imaging," in *2025 International Conference on Modern Sustainable Systems (CMSS)*, Shah Alam, Malaysia, 2025.

[84] K. P, M. K. S, S. P. S and M. T. C, "Deep Learning-Based Gait Analysis from Wearable Sensors for Early Parkinson's Disease Detection," in *2026 International Conference on Intelligent and Innovative Technologies in Computing, Electrical and Electronics (IITCEE)*, Bangalore, India, 2026.

[85] C. D. Pace, A. M. De Nunzio, C. De Stefano, F. Fontanella and M. Molinara, "Markerless Gait Analysis for Parkinson's disease diagnosis: A study on machine learning integration and features explainability," *Engineering Applications of Artificial Intelligence,* vol. 161, p. 112031, 2025.

[86] D. Hemmerling, M. Kaczmarska, B. Krawczyk, M. Dudek, M. Danioł, P. Jemioło, M. Wodziński and M. Wójcik-Pędziwiatr, "Gait analysis in mixed reality for Parkinson's disease assessment," *Biomedical Signal Processing and Control,* vol. 106, p. 107659, 2025.

[87] R. Udhayakumar, S. Gopakumar, S. Rahman and C. Karmakar, "Nonlinear feature space mapping of gait dynamics for neurodegenerative disease detection," *Biomedical Signal Processing and Control,* vol. 107, p. 107800, 2025.

[88] M. Chen, L. Yu, Q. Zhao, X. Wang, E. Hiu, K. Yeung, K. L. Tsui, H. Wang and Y. Zhao, "A data-knowledge driven approach with wearable sensors for intelligent gait disorders identification," *Biomedical Signal Processing and Control,* vol. 111, p. 108289, 2026.

[89] D. G. Boucharas, V. S. Loukas, N. S. Tachos, M. Tsiknakis, G. Manis and D. I. Fotiadis, "A Machine Learning Framework for Parkinson's Disease Detection Through Turning Metrics," in *2025 47th Annual International Conference of the IEEE Engineering in Medicine and Biology Society (EMBC)*, Copenhagen, Denmark, 2025.

[90] S. J. Priya, P. K. Amaladass, S. T. George, M. Subathra and G. N. Sundar, "Recognition of Parkinson disease using Kriging Empirical Mode Decomposition via deep learning techniques," *Gait & Posture,* vol. 122, pp. 85-91, 2025.

[91] M. R. Raja, G. H. Krishnan, A. Mohammad and S. Cheerla, "Dual temporal gated multi-graph convolution network based neurodegenerative disease detection and severity prediction," *Biomedical Signal Processing and Control,* vol. 112, p. 108566, 2026.

[92] M. Mathlouthi, I. H. Trimech and N. E. B. Amara, "Enhanced Multimodal approach for Parkinson's Disease Detection: fusing deep handwriting and Voice Features with Optimized Classification," in *1th International Conference on Control, Decision and Information Technologies,* Split, Croatia, 2025.

[93] M. Ji, H. Dong, L. Guo and W. Li, "Diagnosis and Severity Rating of Parkinson's Disease Based on Multimodal Gait Signal Analysis With GLRT and ST-CNN-Transformer Networks," *IEEE Journal of Translational Engineering in Health and Medicine,* vol. 13, pp. 450-460, 2025.

[94] M. Mathlouthi, I. H. Trimech and N. E. B. Amara, "Enhanced Multimodal approach for Parkinson's Disease Detection: fusing deep handwriting and Voice Features with Optimized Classification," in *2025 11th International Conference on Control, Decision and Information Technologies (CoDIT)*, Split, Croatia, 2025.

[95] A. K. Rastogi, A. K. Singh and R. Srivastava, "Advanced Multimodal Acoustic Data Pre-Processing and Deep Learning Techniques for Enhanced Parkinson's Disease Detection and Management," in *2025 12th International Conference on Computing*

for Sustainable Global Development (INDIACom), Delhi, India, 2025.

[96] N. Aggarwal, B. S. Saini and S. Gupta, "A multi-layered stacked classifier developed for diagnosis of Parkinson's disease and SWEDD patients using fusion of multimodal data," *Biomedical Signal Processing and Control,* vol. 108, p. 107924, 2025.

[97] K. Kumar and R. Ghosh, "A multi-modal Parkinson's disease diagnosis system from EEG signals and online handwritten tasks using grey wolf optimization based deep learning model," *Biomedical Signal Processing and Control,* vol. 100, p. 106946, 2025.

[98] N. Singh, P. tripathi and A. K. Kohat, "IHMF-PD: An interpretable holistic multimodal framework for classifying Parkinson's disease severity," *Biomedical Signal Processing and Control,* vol. 113, p. 108872, 2026.

[99] S. Shanthini and A. Chandrasekar, "Multimodal Parkinson's disease classification using voice signals and hand-drawn images based on deep learning enabled by chronological tangent search optimization," *Biomedical Signal Processing and Control,* vol. 102, p. 107274, 2025.

[100] V. Kukreja, V. Ahuja, M. Ati, H. Shanmugasundaram, M. Krishnamoorthy, R. Sharma and A. Bhattacherjee, "A spatio-temporal fusion-based approach for multi-dimensional classification of Parkinson's disease progression using multi-modal dataset," *Results in Engineering,* vol. 26, p. 105317, 2025.

[101] N. Chowdhury, U. K. Das, S. Sazzad, A. Chowdhury and P. Das, "Multimodal approach for early diagnosis of Parkinson's disease using PET imaging, tremor detection, and machine learning," *Psychiatry Research: Neuroimaging,* vol. 353, p. 112063, 2025.

[102] A. Ivanova, A. Shcherbak, S. Nesteruk, E. Bril, A. Baldycheva and A. Somov, "Parkinson's Disease detection through multimodal data analysis," *Smart Health,* vol. 38, p. 100618, 2025.

[103] G. S. Chakraborty, J. C. Bortty, J. Das, I. R. Noman, K. K. Bishnu and A. Islam, "Efficient multi-modal fusion framework with advanced AI-driven approaches for automated Parkinson's disease detection," *Intelligence-Based Medicine,* vol. 12, p. 100310, 2025.

[104] K. D. S. K, S. S, V. K, D. Y and S. D. V. S, "Diagnosis of Parkinson Disease based on Feature Extraction and ML Techniques," in *2025 IEEE International Conference on Intelligent Signal Processing and Effective Communication Technologies (INSPECT)*, Gwalior, India, 2025.

[105] C. H. Reddy, M. Kanchana and N. M. Reddy, "Enhanced Efficient Diagnosis System for Parkinson's Disease using Hybrid Deep Neural Network," in *2025 International Conference on Emerging Technologies in Engineering Applications (ICETEA)*, Puducherry, India, 2025.

[106] M. Hammoud, A. Shcherbak, E. Bril, M. Semenov, O. Sergiyenko and A. Somov, "Transfer learning for assessing Parkinson's disease: Analysis of wrist-worn sensors data and time-series imaging," *Measurement,* vol. 262, p. 120052, 2026.

[107] R. Singh, Y. Malhotra and J. Parikh, "Integrative approach for early detection of Parkinson's disease and atypical Parkinsonian syndromes leveraging hemodynamic parameters, motion data & advanced AI models," *Computer Methods and Programs*

in Biomedicine, vol. 271, p. 108989, 2025.

[108] A. O. Esan, D. B. Olawade, A. A. Soladoye, B. A. Omodunbi, I. A. Adeyanju and N. Aderinto, "Explainable AI for Parkinson's disease prediction: A machine learning approach with interpretable models," *Current Research in Translational Medicine,* vol. 73, p. 103541, 2025.

[109] S. Sahana, S. Swetha, A. Jenifer and M. Revathi, "Parkinson's Disease Prediction by Voice and Handwritings Using ML & DL," in *2025 9th International Conference on Computational System and Information Technology for Sustainable Solutions (CSITSS)*, Bangalore, India, 2025.

[110] Al-Amain, M. N. Saad and R. Bardhan, "Balanced vs. Imbalanced Data in Parkinson's Disease Detection: A Machine Learning, Ensemble Machine Learning and Deep Learning Perspective Using SMOTE Based on Clinical Data," in *2025 International Conference on Electrical, Computer and Communication Engineering (ECCE)*, Chattogram, Bangladesh, 2025.

[111] M. Nagaraju, K. L. Madhuri, D. Snehalatha and S. Sawant, "Analysis of Electromyography Wearable Sensors and Deep Learning Algorithms used in Parkinson's Diagnosis," in *2025 10th International Conference on Communication and Electronics Systems (ICCES)*, Coimbatore, India, 2025.

[112] L. Jarod, N. Shehata, I. Singh, A. Hyun and G. Kahanda, "The Utilization of An Artificial Intelligence and Machine Learning Model to Aid in Accelerating Parkinson's Disease Diagnosis," in *2025 International Conference on Artificial Intelligence, Computer, Data Sciences and Applications (ACDSA)*, Antalya, Türkiye, 2025.

[113] J. J. Hathaliya, H. Modi, R. Gupta and S. Tanwar, "Deep learning and Blockchain-based Essential and Parkinson Tremor Classification Scheme," in *IEEE INFOCOM 2022 - IEEE Conference on Computer Communications Workshops (INFOCOM WKSHPS)*, New York, NY, USA, 2022.

[114] C.-T. Wu, C.-C. Hsiao, S.-M. Wang, K.-Z. Su, T.-T. Hsieh, S.-W. Huang, H.-T. Lee, L.-Y. Jhao, J.-C. Cau, H.-J. Chiu, H.-M. Chen and P.-Y. Chiu, "A facial expression-based artificial intelligence model to aid in screening for Parkinson's disease: Development and validation in a cohort study," *Biomedical Signal Processing and Control,* vol. 113, p. 108974, 2026.

[115] O. Pinto Neto and T. O. R. Pinho, "Grip force variability and deep learning: A cross-sectional study of a novel biomarker for early detection of Parkinson's disease," *NeuroMarkers,* vol. 2, p. 100106, 2025.

[116] M. I. Mahali, J.-S. Leu, C. Avian, J. T. Darmawan, M. Faisal, N. A. S. Putro and S. W. Prakosa, "Enhancing tremor classification: Transformer-based analysis of biomechanics patterns for Parkinson's and essential tremor," *Clinical Biomechanics,* vol. 127, p. 106599, 2025.

[117] A. Mumuni and F. Mumuni, "Data augmentation: A comprehensive survey of modern approaches," *Array,* vol. 16, 2022.

[118] A. Mazraeh, "Tabular Data Augmentation: From Basics to Advanced Techniques," 6 3 2025. [Online]. Available: https://medium.com/@adnan.mazraeh1993/data-augmentation-from-basics-to-advanced-concepts-179963c25a9a. [Accessed 25 2 2026].

[119] N. V. Chawla, K. V. Bowyer, L. O. Hall and W. P. Kegelmeyer, "SMOTE: Synthetic Minority Over-sampling Technique," *Journal of Artificial Intelligence Research,* vol. 16, pp. 321-357, 2002.

[120] O. Parise, R. Kronenberger, G. Parise, C. d. asmundis, S. Gelsomino and M. L. Meir, "CTGAN-driven synthetic data generation: A multidisciplinary, expert-guided approach (TIMA)," *Computer Methods and Programs in Biomedicine,* vol. 259, 2025.

[121] Y. Zhao, Y. Cen, S. H. Javaheri, M. M. Sepehri and B. Teimourpour, "Data Normalization," in *Data Mining Applications with R*, Academic Press, 2014, pp. 153-180.

[122] D. Highland and G. Zhou, "A review of detection techniques for depression and bipolar disorder," *Smart Health,* vol. 24, 2022.

[123] S. A. Hicks, I. Strümke, V. Thambawita, M. Hammou, M. A. Riegler, P. Halvorsen and S. Parasa, "On evaluation metrics for medical," *scientific reports,* vol. 12, 2022.

[124] A. Popov, "Feature engineering methods," in *Advanced Methods in Biomedical Signal Processing and Analysis*, Academic Press, 2023, pp. 1-29.

[125] A. Casas-Ordaz, E. H. Haro, L. A. Beltran, O. Alvarez, S. J. Mousavirad, M. Pérez-Cisneros and D. Oliva, "Particle swarm optimization: A survey of innovations over the last 10 years," *Computer Science Review,* vol. 60, 2026.

[126] F. S. Gharehchopogh, A. Ucan, T. Ibrikci, B. Arasteh and G. Isik, "Slime Mould Algorithm: A Comprehensive Survey of Its Variants and Applications," *Archives of Computational Methods in Engineering,* vol. 30, pp. 2683-2723, 2023.

[127] W. Xiong, D. Zhu, R. Li, Y. Yao, C. Zhou and S. Cheng, "An effective method for global optimization – Improved slime mould algorithm combine multiple strategies," *Egyptian Informatics Journal,* vol. 25, p. 100442, 2024.

[128] S. Mirjalili and A. Lewis, "The Whale Optimization Algorithm," *Advances in Engineering Software,* vol. 95, pp. 51-67, 2016.

[129] scikit- learn, "Plot different SVM classifiers in the iris dataset," 19 10 2011. [Online]. Available: https://scikit-learn.org/stable/auto_examples/svm/plot_iris_svc.html. [Accessed 22 7 2026].

[130] scikit learn, "1.6. Nearest Neighbors — scikit-learn 1.9.0 documentation," 19 10 2011. [Online]. Available: https://scikit-learn.org/stable/modules/neighbors.html. [Accessed 22 7 2026].

[131] scikit-learn, "1.10. Decision Trees — scikit-learn 1.9.0 documentation," 19 10 2011. [Online]. Available: https://scikit-learn.org/stable/modules/tree.html. [Accessed 22 7 2026].

[132] scikit-learn, "RandomForestClassifier — scikit-learn 1.9.0 documentation," 19 10 2011. [Online]. Available: https://scikit-learn.org/stable/modules/generated/sklearn.ensemble.RandomForestClassifier.html. [Accessed 23 7 2026].

[133] scikit-learn, "1.9. Naive Bayes — scikit-learn 1.9.0 documentation," 19 10 2011. [Online]. Available: https://scikit-learn.org/stable/modules/naive_bayes.html. [Accessed 23 7 2026].

[134] scikit-learn, "LogisticRegression — scikit-learn 1.9.0 documentation," 19 10 2011. [Online]. Available: https://scikit-

learn.org/stable/modules/generated/sklearn.linear_model.LogisticRegression.html. [Accessed 23 7 2026].

[135] xgboost, "Python Package Introduction — xgboost 3.3.0 documentation," 19 10 2011. [Online]. Available: https://xgboost.readthedocs.io/en/stable/python/python_intro.html#setting-parameters. [Accessed 23 7 2026].

[136] Medium, "Recurrent Neural Networks (RNNs) and Long Short-Term Memory (LSTM) — Creating an LSTM Model in Python Using TensorFlow and Keras | by TechwithJulles | Medium," 13 10 2024. [Online]. Available: https://medium.com/@techwithjulles/recurrent-neural-networks-rnns-and-long-short-term-memory-lstm-creating-an-lstm-model-in-13c88b7736e2. [Accessed 23 7 2026].